BY-NC

Mirosław Łomozik

Microstructure, Toughness and Hardness of a Simulated HAZ in Steel S1100QL and of the HAZ of an Actual MAG-Welded Joint Made Using a Metallic Flux-Cored Wire

Abstract: Simulation tests discussed in the article involved structural steel S1100QL having a yield point of more than 900 MPa. The simulations included single (T_{max} = 1250°C) and double welding thermal cycle (T_{max} = 1250°C + 600°C, T_{max} = 1250°C + 760°C and T_{max} = 1250°C + 900°C) as well as cooling times $t_{8/5}$ = 3, 5 and 10 s. Specimens with the simulated heat affected zone (HAZ) were subjected to impact strength tests performed at a temperature of -40°C and +20°C, Vickers hardness tests (HV10) and microscopic metallographic tests (involving light microscopy). Test results were presented in diagrams and photographs. Related comparisons included results of the structural, hardness and toughness tests of simulated HAZs with analogous results obtained during the actual repair welding of a MAG-welded joint made of steel S1100QL. The final part of the article contains discussion concerning the test results and the statement concerning the obtainment of the significant conformity of the phase composition and the morphology of the microstructure as well as the average hardness values of the HAZ areas obtained in the simulations and those of the HAZ area obtained in the actual welded joint. In relation to all tested simulation variants, the impact energy of the simulated HAZ area of steel S1100QL satisfied the minimum criterion of KV = 27 J both in relation to a test temperature of -40°C and that of +20°C. The number of repeated (1 through 4) thermal cycles having preset parameters did not trigger explicitly noticeable changes in impact energy values as regards the simulated HAZ of steel S1100QL.

Keywords: steel S1100QL, heat affected zone (HAZ), simulation tests, metallographic tests, hardness, toughness

DOI: *10.17729/ebis.2021.5/5*

Introduction

The continuous development of steel structures results in their ever growing complexity, dimensions and performance requirements. At the same time, design engineers and manufacturers aim at the reduction of structure weight and fabrication costs. These contradictory requirements can only be satisfied by structural steels characterised by high and very high mechanical properties [1–3]. As a result, designers and

dr hab. inż. Mirosław Łomozik – Łukasiewicz Research Network – Instytut Spawalnictwa, Research Group for Materials Weldability and Welded Structures

BY-NC

design engineers continue to be interested in toughened steels characterised by high and very high strength and low nil ductility transition temperature.

Several producers, e.g. SSAB Oxelösund, Sweden, offer steel grades having a yield point of more than 900 MPa [4, 5]. High-strength martensitic steels are very attractive structural materials, yet welding such steels poses some problems. A heat input to the joint during the welding process is responsible for the local deterioration of mechanical properties in the heat affected zone (HAZ).

The authors of publication [6] presented tests results concerning the effect of a heat input on the microstructure of single-run joints made of steel S1100QL. The above-named joints were made using the MAG method and a Union X 90 filler metal wire (Thyssen) (enabling the obtainment of weld deposit having a yield point of 900 MPa). The authors of the aforesaid work stated that the key factor affecting the microstructure and properties of single-run joints made of steel S1100QL, i.e. a heat input, should be as low as possible. A higher heat input to the joint was responsible for the formation of the coarse-grained structure in the HAZ and the reduction of martensite hardness, which, in turn, led to the deterioration of the mechanical properties of the joint in comparison with those characteristic of the base material of steel S1100QL. Articles [7–9] discuss works concerning the development of new filler metals characterised by very high strength. Presently, there is no information concerning the multiple effect of welding thermal cycles on the microstructure and properties of welded joints made of steels having a yield point of more than 900 MPa (as is the case with repair welding).

This article discusses results of tests concerning the effect of multiple welding thermal cycles on the microstructure and mechanical properties of simulated HAZ areas in steel S1100QL and those of the actual joint made of the aforesaid steel, subjected to repeated repair.

Table 1. Chemical composition of steel S1100QL

Chemical element content, % by weight									
C	Si	Mn	P	S	Cr	Mo	Ni	Cu	B
0.192	0.220	0.855	0.014	0.0034	0.606	0.636	1.858	0.012	0.0017
Chemical element content, % by weight – according to the producer [10]									
C	Si	Mn	P	S	Cr	Mo	Ni	Cu	B
max. 0.21	max. 0.50	max. 1.40	max. 0.020	max. 0.005	max. 0.80	max. 0.70	max. 3.00	max. 0.30	max. 0.005

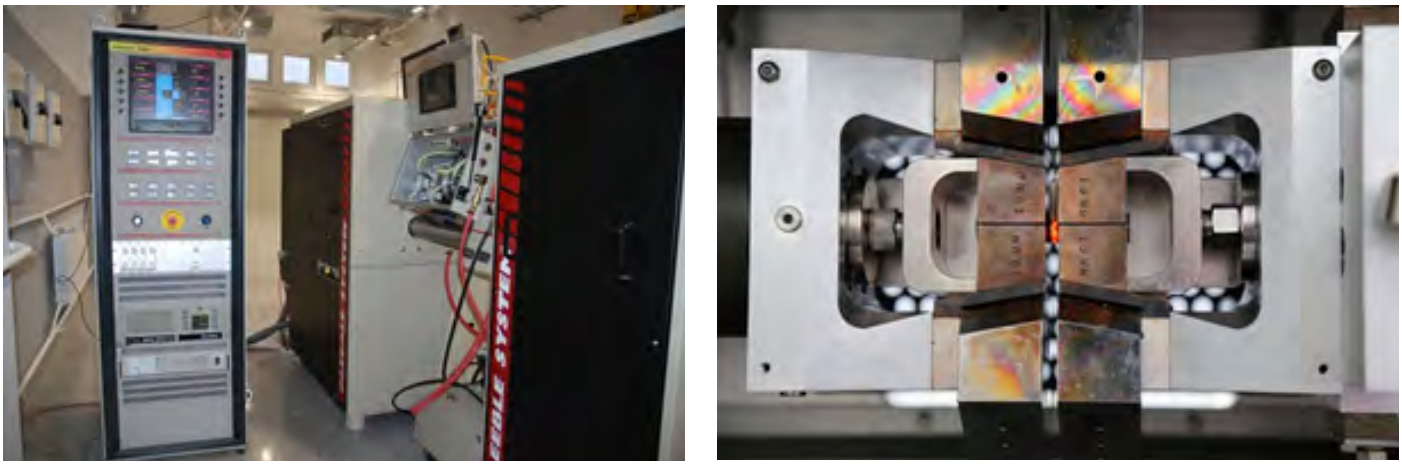

Fig. 1. Gleeble 3500 simulator at Łukasiewicz – Instytut Spawalnictwa: a) main view and b) specimen fixed in the current clamps of the simulator

BY-NC

Test materials

The tests discussed in the article involved 18 mm thick plates made of high-strength toughened steel S1100QL. The analysis of the chemical composition of steel grade S1100QL was performed using a Q4 TASMAN 170 spark emission spectrometer (Bruker; Germany). The analysis results are presented in Table 1.

Testing methodology

Simulation tests

The image of the simulated HAZ in the test steel was obtained using a Gleeble 3500 simulator of thermal and strain cycles (DSI; USA) (Fig. 1). The simulation tests involved the use of impact specimens having dimensions 10 mm × 10 mm × 55 mm.

The simulation required the identification of critical temperatures AC1 and AC3 in relation to steel S1100QL. The above-named temperatures were determined using the following equations [11, 12]:

$$A_{C1} = 723 - 10.7xMn - 16.9xNi + 29.1xSi + 16.9xCr + 290xAs + 6.38xW \quad [1]$$

$$A_{C3} = 910 - 203xC1/2 - 15.2xNi + 44.7xSi + 104xV + 31.5xMo + 13.1xW - (30xMn + 11xCr + 20xCu - 700xP - 400xAl - 120xAs - 400xTi) \quad [2]$$

The use of the chemical element contents (presented in Table 1) in equations [1] and [2] enabled the identification of critical temperature values in relation to steel S1100QL, i.e. A_{C1} = 700°C and A_{C3} = 828°C.

The idea of the programme, presented in Table 2, was to simulate thermal conditions during the actual MAG welding of steel S1100QL involving the single and double effect of the welding thermal cycle.

Impact strength tests

After the simulation, 2 mm deep Charpy V type notches were made centrally in the HAZ. The impact tests were performed at a temperature

Table 2. Simulation parameters

Single thermal cycle	
T_{max}, °C	$t_{8/5}$, s
1250	3
	5
	10

Double thermal cycle		
T_{max1}, °C	T_{max2}, °C	$t_{8/5}$, s
1250	600 (below temperature A_{C1})	5
		10
	760 (between A_{C1}-A_{C3})	5
		10
	900 (above temperature A_{C3})	5
		10

Where
a) T_{max} – maximum temperature of the welding thermal cycle,
b) $t_{8/5}$ – time of HAZ cooling between 800°C and 500°C,
c) A_{C1}, A_{C3} – critical temperatures,
d) number of thermal cycle repetitions: 1, 2, 3 and 4 times (where 1 – simulation of production welding and 2, 3 and 4 – simulations of the first, second and third repair welding respectively).

BY-NC

of -40°C and +20°C (in accordance with the requirements of standard PN-EN ISO 148-1 [13]) using an Amsler RPK 300 impact testing machine (Germany).

Microscopic metallographic tests of simulated HAZ areas

Metallographic specimens (for microscopic tests) prepared on simulated HAZ areas were subjected to light microscopy-based tests (in accordance with the requirements of the PN-EN ISO 17639 standard) [14]. The microstructure of the specimens was revealed through Nital-based chemical etching. The microscopic tests were performed using a Nikon Eclipse MA 200 optical metallographic inverted microscope (Nikon; Japan) and NIS Elements-AR measurement software (Nikon).

Hardness measurements of simulated HAZ areas

The simulated HAZ areas were subjected to Vickers hardness tests performed using a KB-50BVZ-FA automatic hardness tester (Prüftechnik GmbH; Germany) and a penetrator load of 98.1 N (HV10) (in accordance with the requirements of the PN-EN ISO 6507-1 standard) [15].

Welded joint subjected to quadruple repair

A test joint (400 mm × 150 mm × 18 mm) was made of steel S110QL using a STEIN-MEGAFIL 1100 M metallic flux-cored (process 138; EN ISO 18276-A classification - T 89 4 Mn2Ni1CrMo M M 1 H5). The filler metal wire diameter amounted to 1.2 mm. The shielding gas used in the process was ISO 14175 - M21 - ArC-18. The root layer was welded using a Lincoln Power WAVE 455 STT semiautomatic welding machine, whereas filling layers were made using a Multi Surfacer D2 mechanised welding station (Welding Alloys). The schematic diagram of the welded joint is presented in Figure 2.

The fabrication cycle used when making the test joint subjected to quadruple repair was the following: the making of a production joint, the performance of non-destructive tests, the removal of the weld using arc-air gouging + the performance of the 1-st repair, the performance of non-destructive tests, the removal of the weld + the performance of the 2-nd repair, the performance of non-destructive tests, the removal of the weld + the performance of the 3-rd repair, the performance of non-destructive tests, the removal of the weld and the making of another, i.e. 4-th repair weld.

Afterwards, the repair joint was subjected to destructive tests (impact strength test, hardness measurements and microscopic metallographic tests). The macrostructure of the repair welded joint as well as the microstructure of its individual areas were identified using Nital-based chemical etching.

The impact strength tests of the welded joint involved impact specimens having dimensions of 10 mm × 10 mm × 55 mm. The tests were performed at a temperature of -40°C, in accordance with the requirements of the PN-EN ISO 9016 standard [16]. In turn, impact strength tests were performed in accordance with the requirements of the PN-EN ISO 9015-1 standard [17], along three measurement lines located

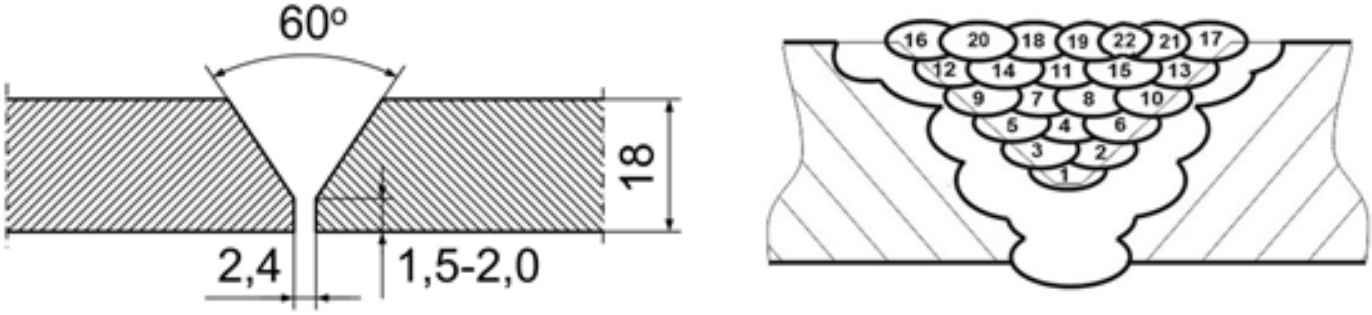

Fig. 2. Shape and dimensions of the weld grove a) and the welding sequence in the repaired joint b)

BY-NC

near the weld face, at the half of the joint thickness and near the weld root.

Test results

Microscopic metallographic tests of simulated HAZ areas

The results of the microscopic metallographic tests of the base material of steel S1100QL are presented in Figure 3. In turn, results concerning the simulated HAZ areas of steel S1100QL are presented in Figures 4–12.

Impact strength tests

Impact energy test results concerning all simulation variants and numbers of welding thermal cycles are presented in Figures 13–16.

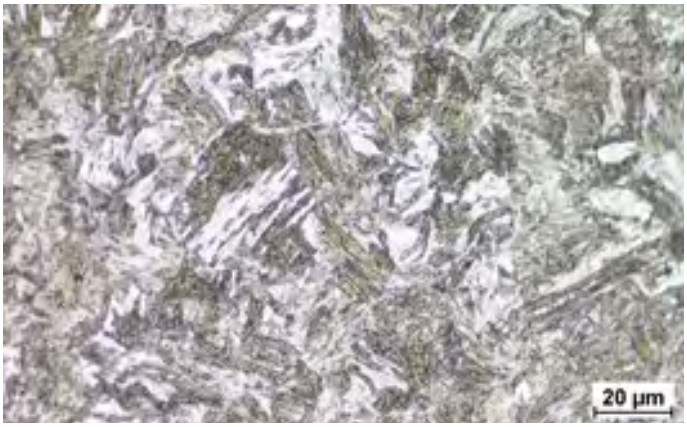

Fig. 3. Base material of steel S1100QL: martensite, hardness: 430 HV10av., mag. 500x

Measurements of the hardness of simulated HAZ areas

Hardness measurement results concerning all simulation variants and numbers of welding thermal cycles are presented in Figures 17 and 18.

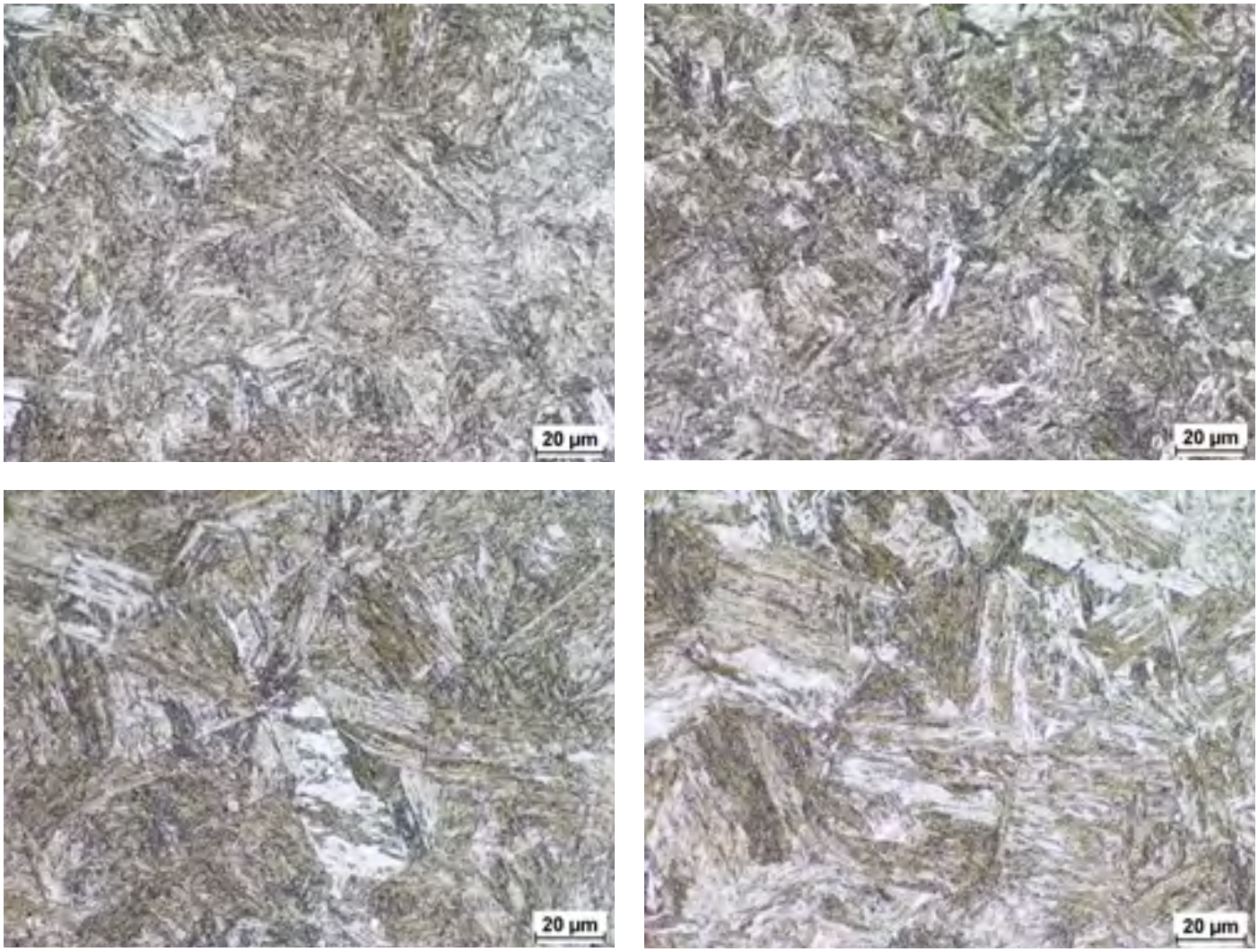

Fig. 4. Microstructure of steel S1100QL after simulation involving one thermal cycle in relation to cooling time t8/5 = 3 s: a) heating 1x, martensite, hardness: 445 HV10av., mag. 500x, b) heating 2x, martensite, hardness 453 HV10av., mag. 500x, c) heating 3x, martensite, hardness 383 HV10av., mag. 500x and d) heating 4x, martensite, hardness 435 HV10av., mag. 500x

BY-NC

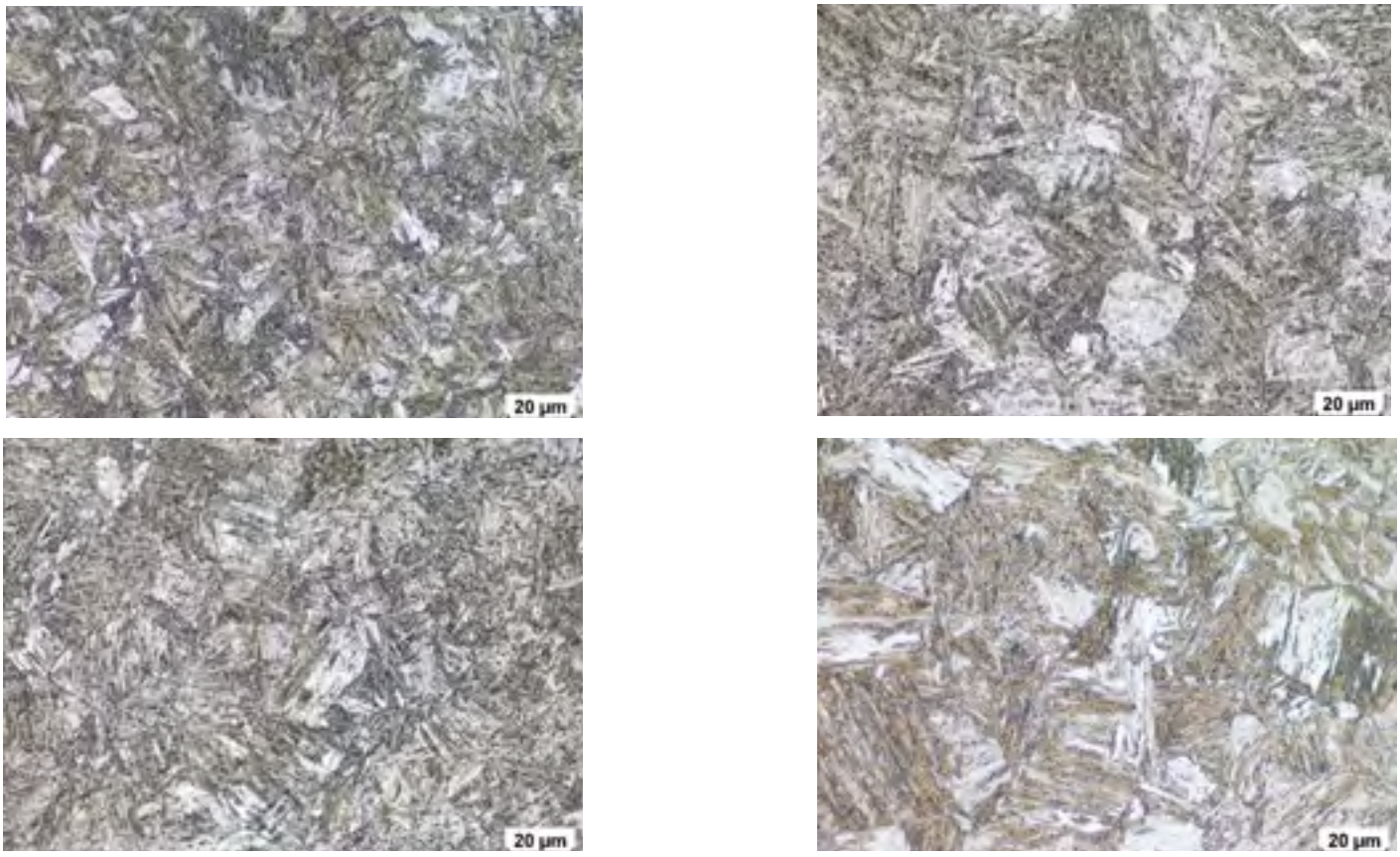

Fig. 5. Microstructure of steel S1100QL after simulation involving one thermal cycle in relation to cooling time t8/5 = 5 s: a) heating 1x, martensite, hardness: 450 HV10av., mag. 500x, b) heating 2x, martensite, hardness: 454 HV10av., mag. 500x, c) heating 3x, martensite, hardness: 396 HV10av., mag. 500x and d) heating 4x, martensite, hardness: 434 HV10av., mag. 500x

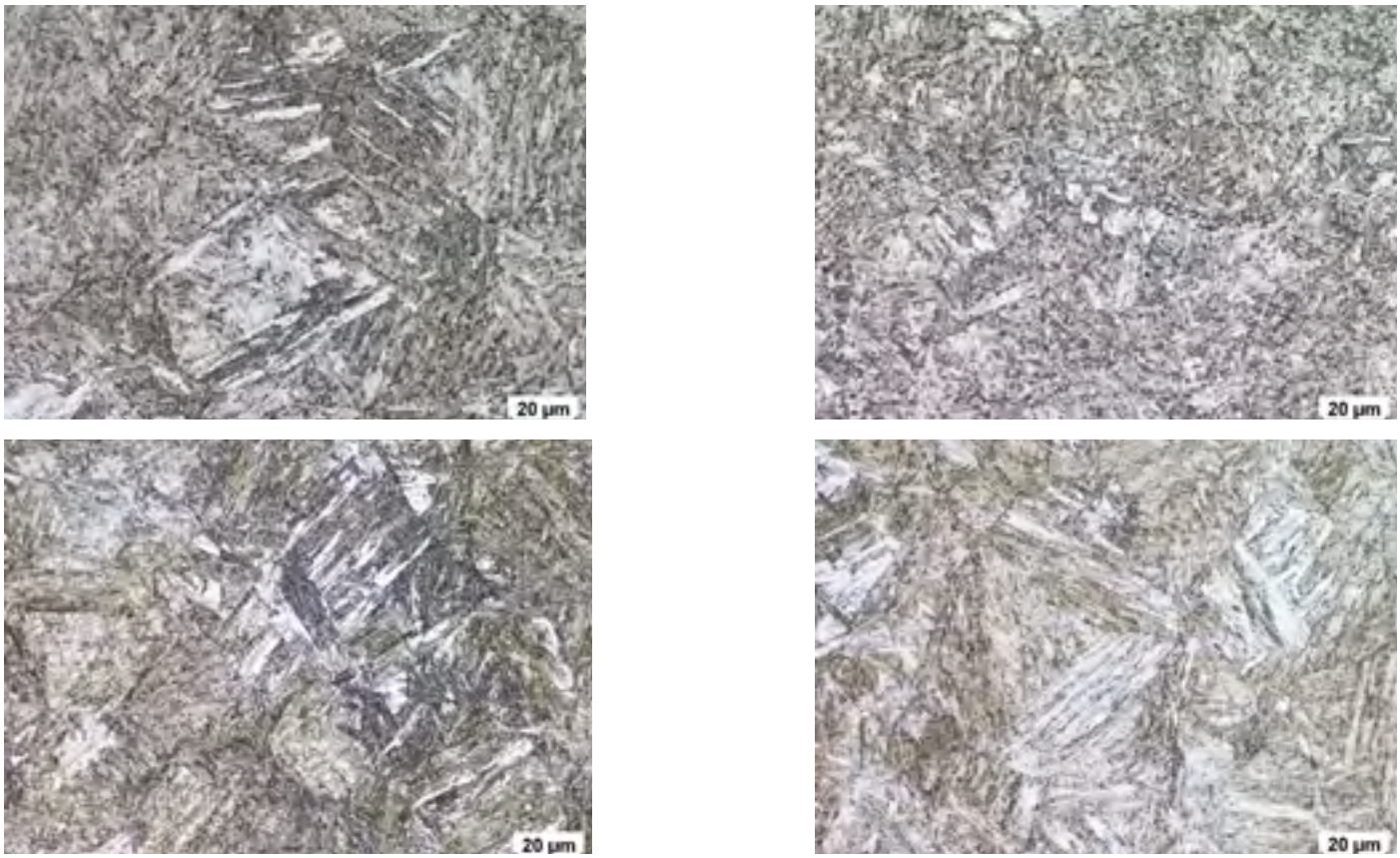

Fig. 6. Microstructure of steel S1100QL after simulation involving one thermal cycle in relation to cooling time t8/5 = 10 s: a) heating 1x, martensite, hardness: 458 HV10av., mag. 500x, b) heating 2x, martensite, hardness: 406 HV10av., mag. 500x, c) heating 3x, martensite, hardness: 442 HV10av., mag. 500x and d) heating 4x, martensite, hardness: 442 HV10av., mag. 500x

BY-NC

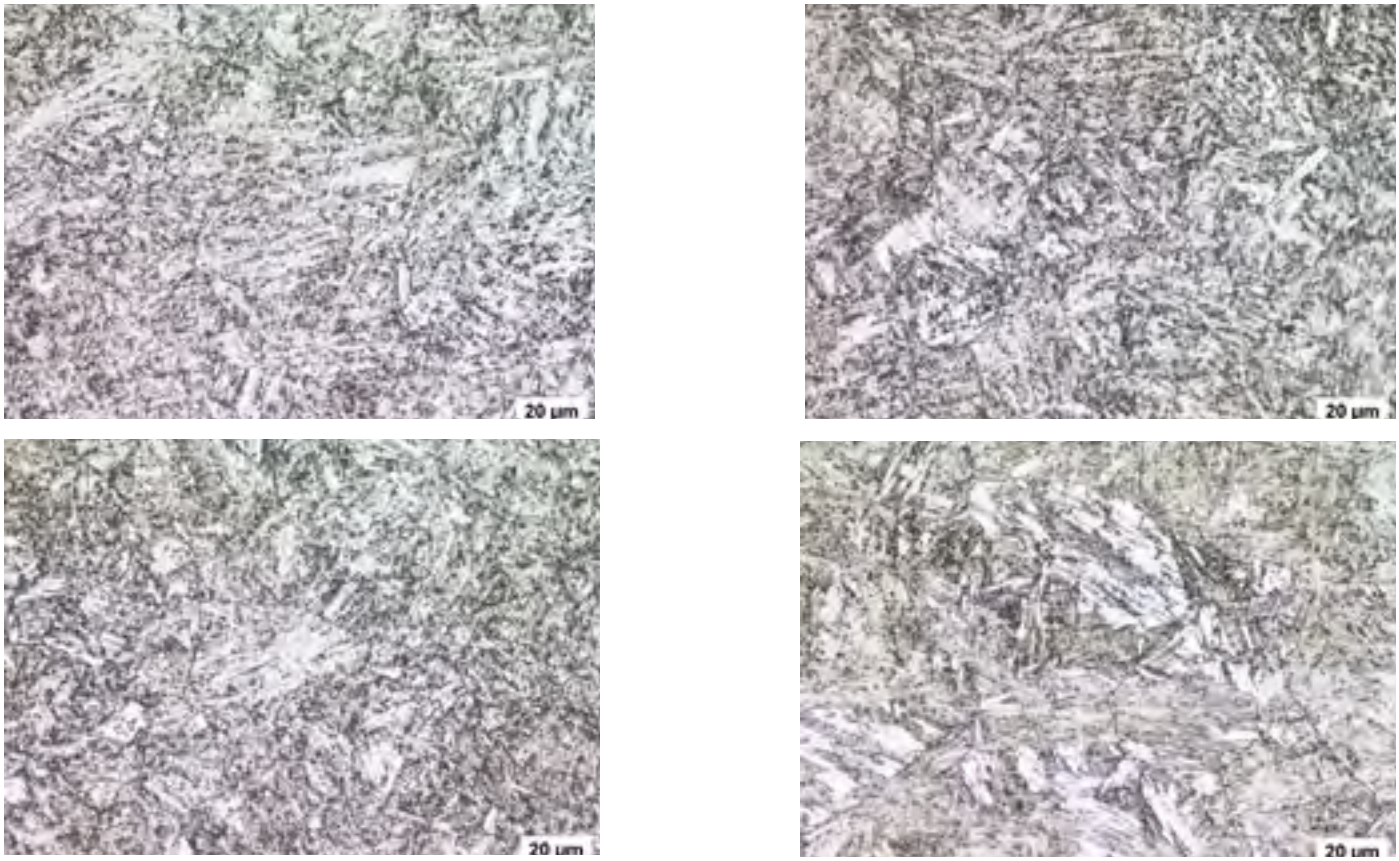

Fig. 7. Microstructure of steel S1100QL after simulation involving double thermal cycle (Tmax1 = 1250°C + Tmax2 = 600°C) in relation to cooling time t8/5 = 5 s: a) heating 1x, bainite and small amounts of ferrite, hardness: 330 HV10av., mag. 500x, b) heating 2x, bainite and ferrite, hardness: 358 HV10av., mag. 500x, c) heating 3x, bainite and small amounts of ferrite, hardness: 328 HV10av., mag. 500x and d) heating 4x, bainite and ferrite, hardness: 381 HV10av., mag. 500x

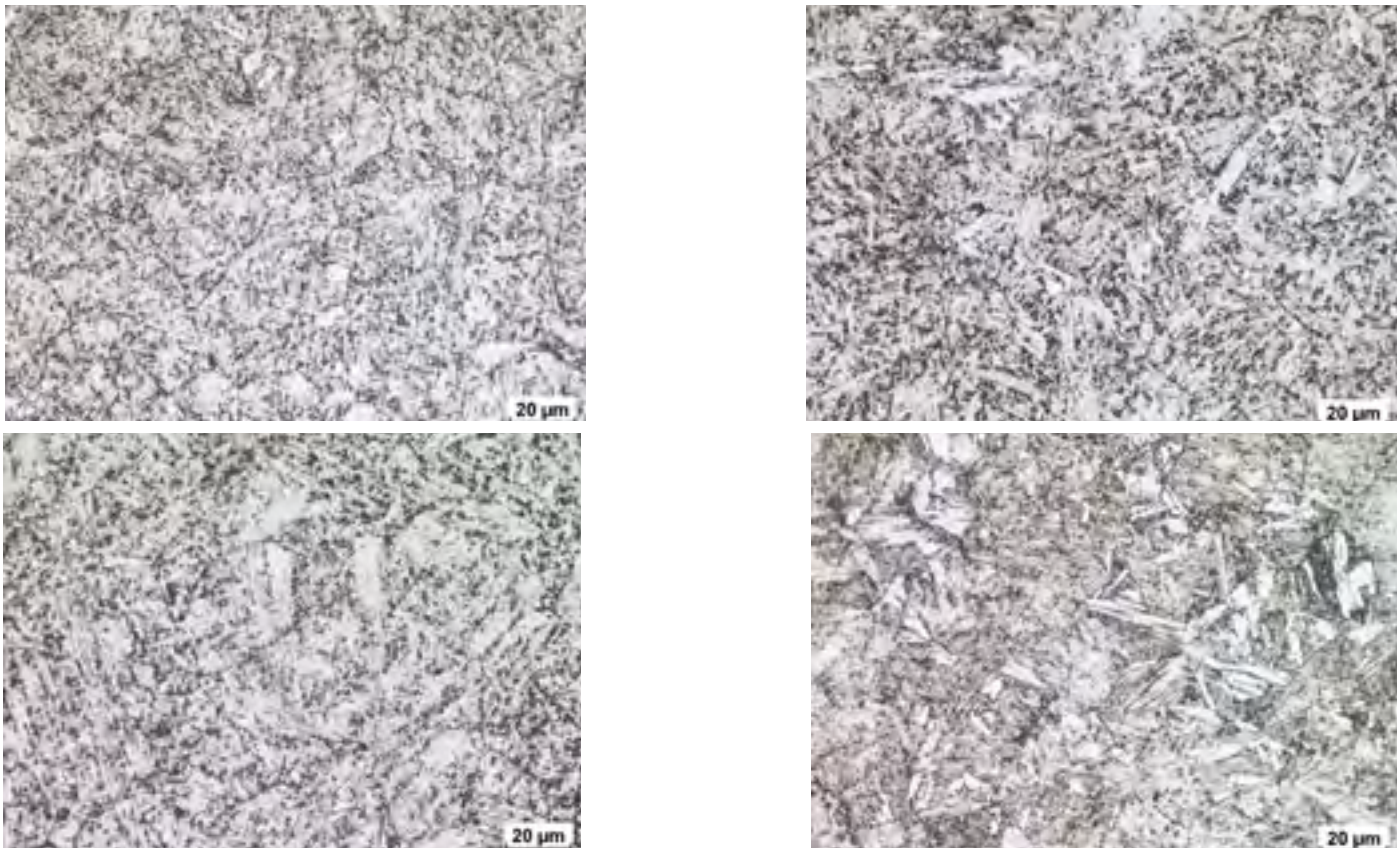

Fig. 8. Microstructure of steel S1100QL after simulation involving double thermal cycle (Tmax1 = 1250°C + Tmax2 = 600°C) in relation to cooling time t8/5 = 10 s: a) heating 1x, bainite and traces of ferrite, hardness: 368 HV10av., mag. 500x, b) heating 2x, bainite and small amounts of ferrite, hardness: 375 HV10av., mag. 500x, c) heating 3x, bainite, hardness: 360 HV10av., mag. 500x and d) heating 4x, bainite and ferrite, hardness: 377 HV10av., mag. 500x

BY-NC

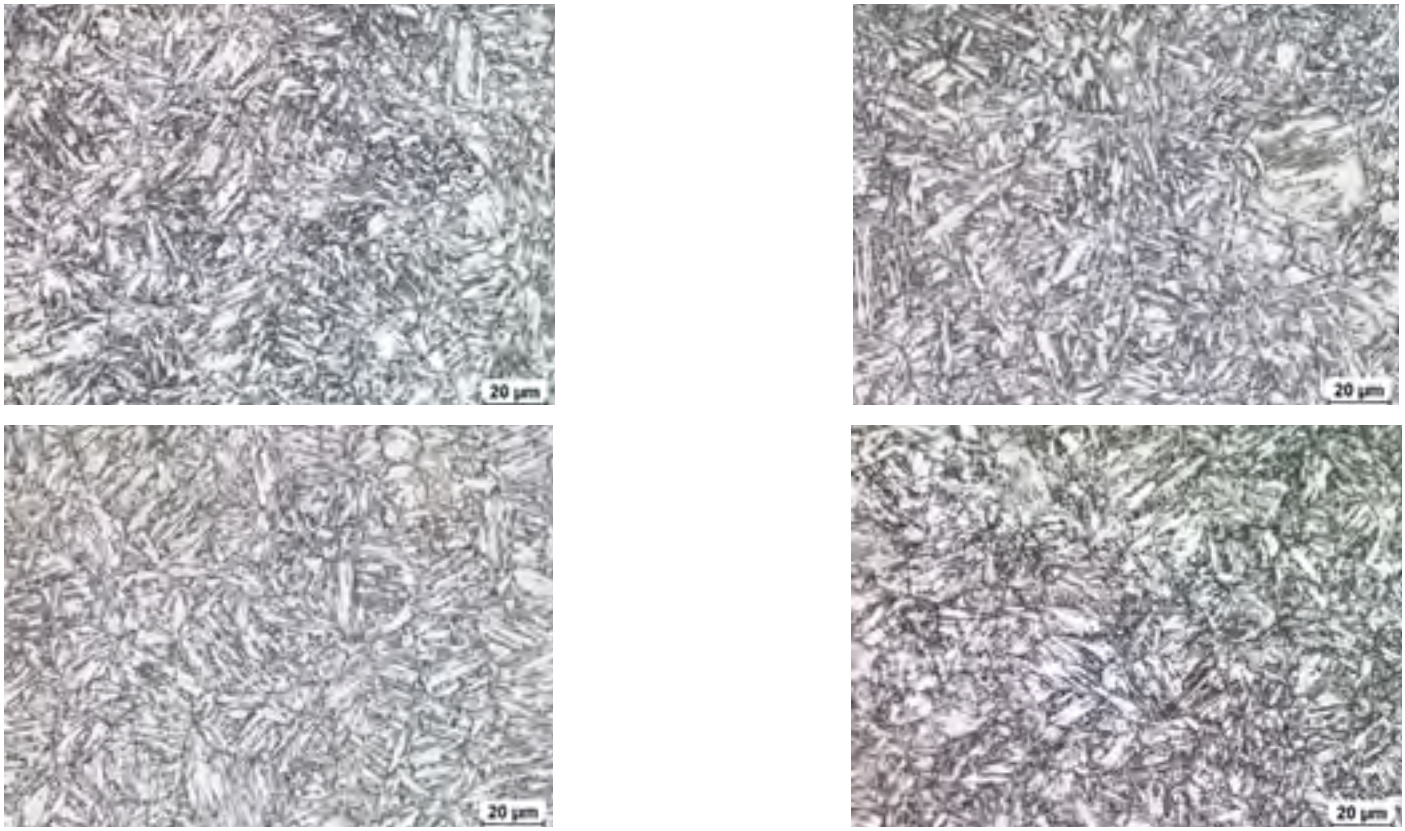

Fig. 9. Microstructure of steel S1100QL after simulation involving double thermal cycle (Tmax1 = 1250°C + Tmax2 = 760°C) in relation to cooling time t8/5 = 5 s: a) heating 1x, mixture of bainite and ferrite, hardness: 348 HV10av., mag. 500x, b) heating 2x, mixture of bainite and ferrite, hardness: 352 HV10av., mag. 500x, c) heating 3x, mixture of bainite, "fresh" martensite and ferrite, hardness: 343 HV10av., mag. 500x and d) heating 4x, mixture of bainite, "fresh" martensite and ferrite, hardness: 355 HV10av., mag. 500x

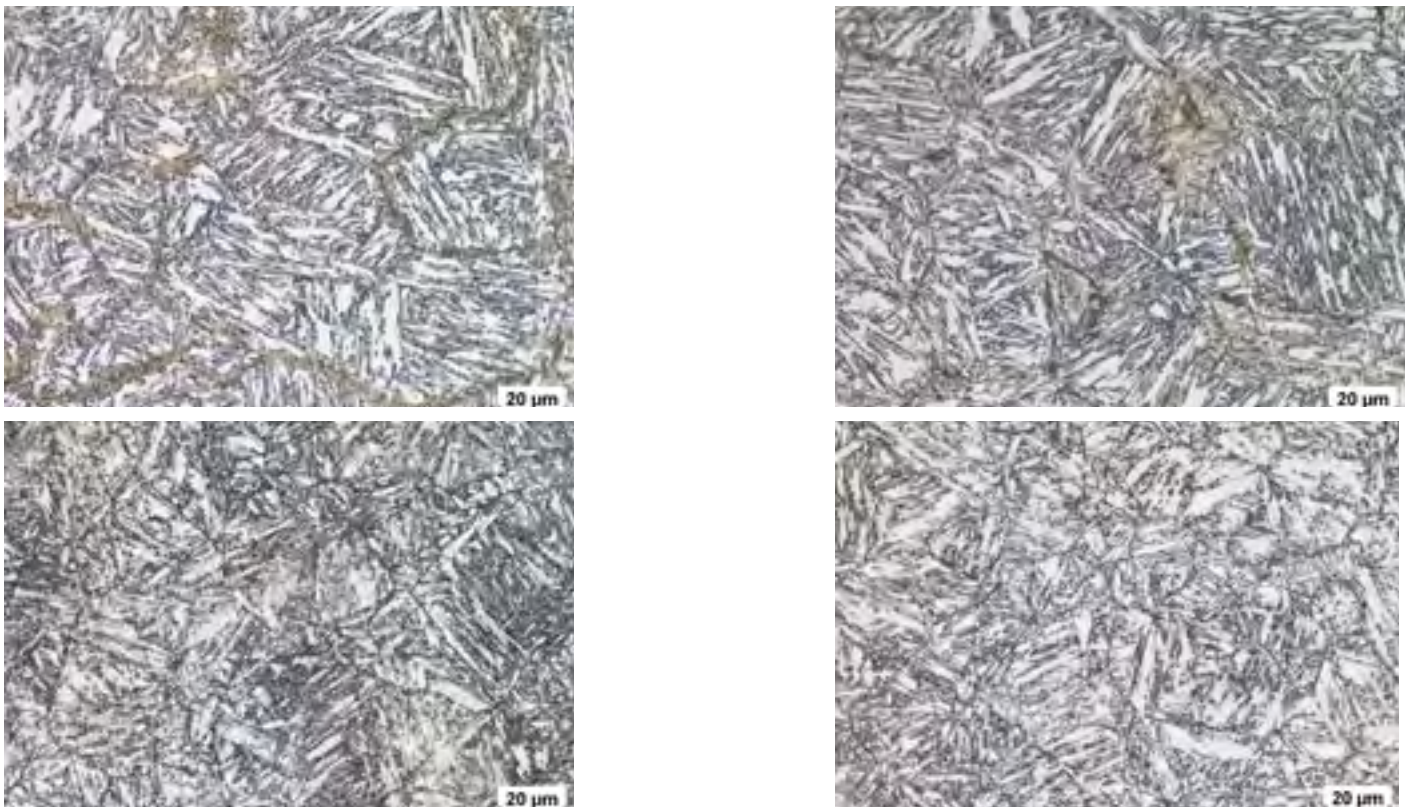

Fig. 10. Microstructure of steel S1100QL after simulation involving double thermal cycle (Tmax1 = 1250°C + Tmax2 = 760°C) in relation to cooling time t8/5 = 10 s: a) heating 1x, high-tempered martensite and "fresh" martensite, hardness: 366 HV10av., mag. 500x, b) heating 2x, high-tempered martensite and "fresh" martensite, hardness: 325 HV10av., mag. 500x, c) heating 3x, mixture of bainite, martensite and a small amount of ferrite, hardness: 346 HV10av., mag. 500x and d) heating 4x, mixture of bainite, martensite and ferrite, hardness: 383 HV10av., mag. 500x

BY-NC

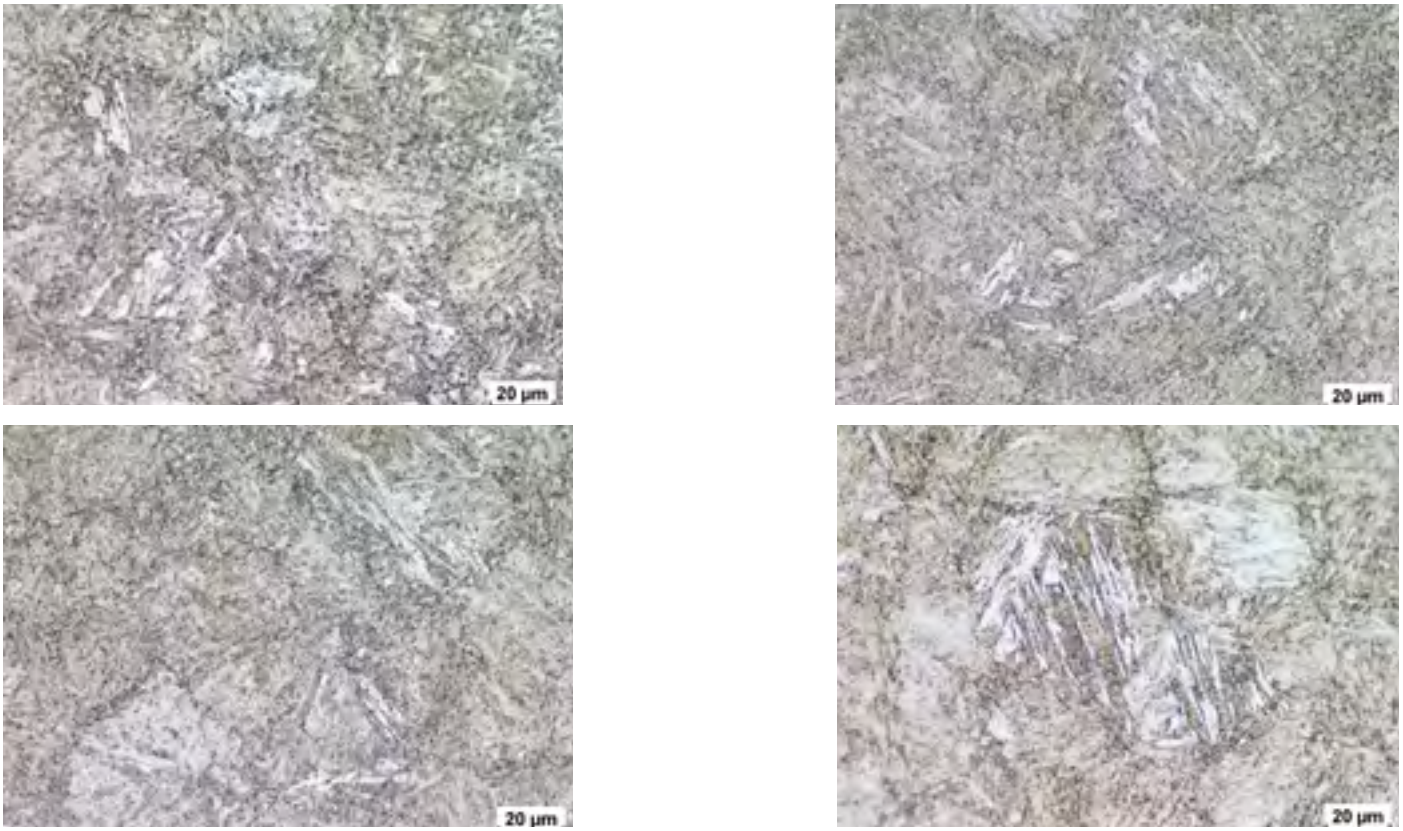

Fig. 11. Microstructure of steel S1100QL after simulation involving double thermal cycle (Tmax1 = 1250°C + Tmax2 = 900°C) in relation to cooling time t8/5 = 5 s: a) heating 1x, mixture of bainite, martensite and ferrite, hardness: 355 HV10av., mag. 500x, b) heating 2x, mixture of bainite, martensite and ferrite, hardness: 454 HV10av., mag. 500x, c) heating 3x, mixture of bainite, martensite and ferrite, hardness: 391 HV10av., mag. 500x and d) heating 4x, mixture of bainite, martensite and ferrite, hardness: 426 HV10av., mag. 500x

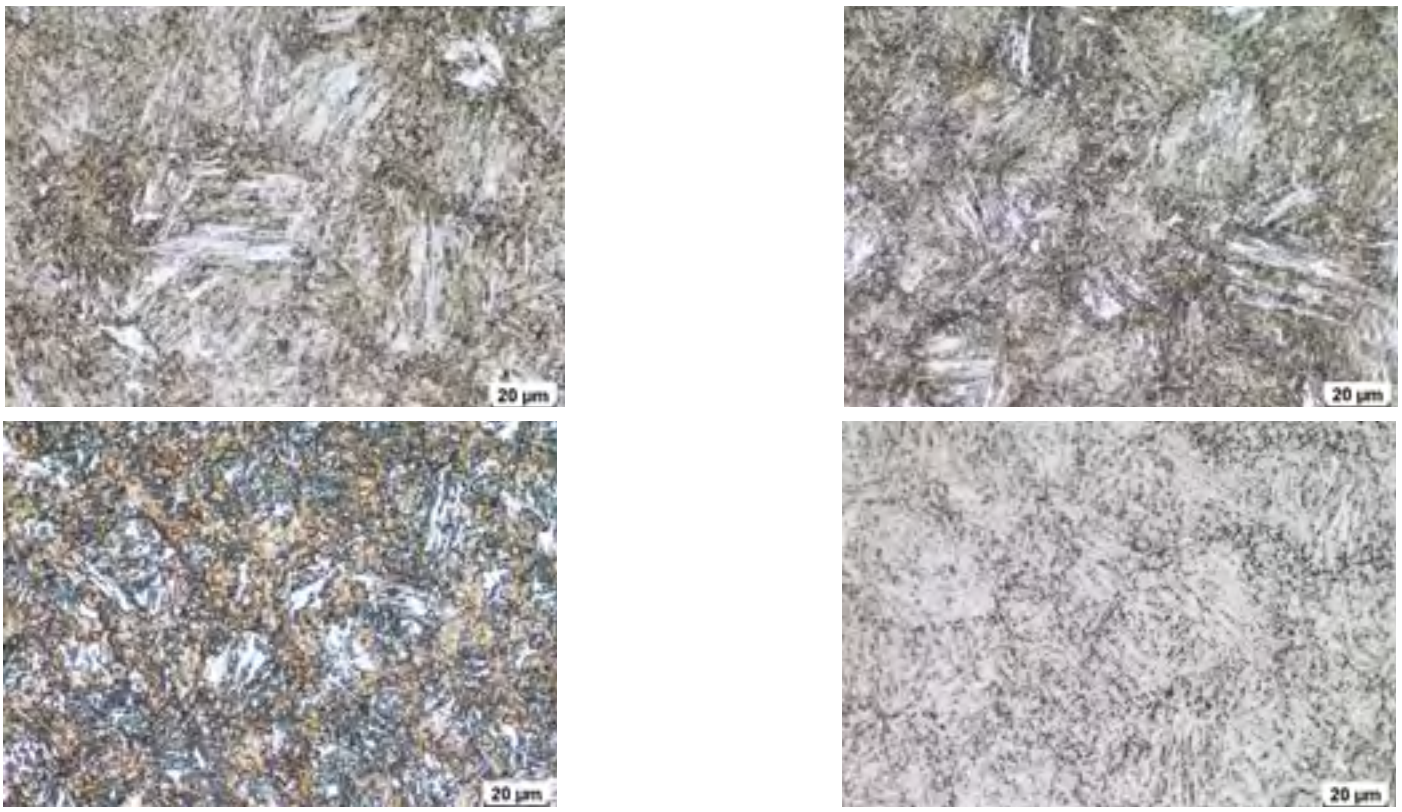

Fig. 12. Microstructure of steel S1100QL after simulation involving double thermal cycle (Tmax1 = 1250°C + Tmax2 = 900°C) in relation to cooling time t8/5 = 10 s: a) heating 1x, mixture of bainite, martensite and ferrite, hardness: 449 HV10av., mag. 500x, b) heating 2x, mixture of bainite, martensite and ferrite, hardness: 412 HV10av., mag. 500x, c) heating 3x, mixture of bainite, martensite and ferrite, hardness: 428 HV10av., mag. 500x and d) heating 4x, mixture of bainite, martensite and a small amount of ferrite, hardness: 453 HV10av., mag. 500x

BY-NC

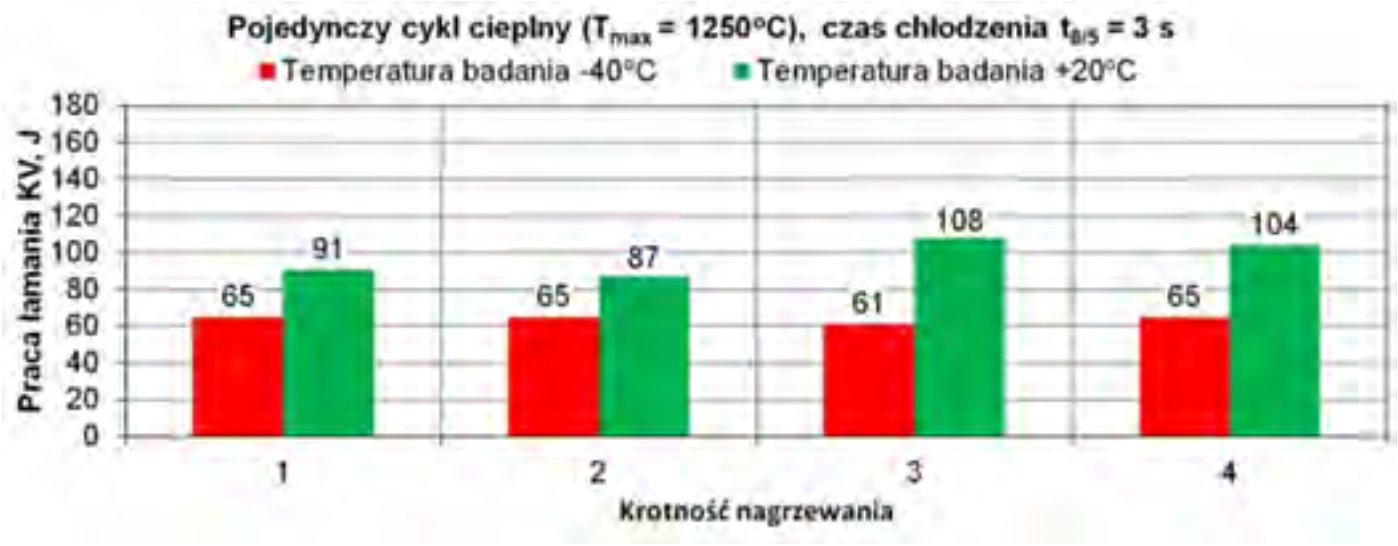

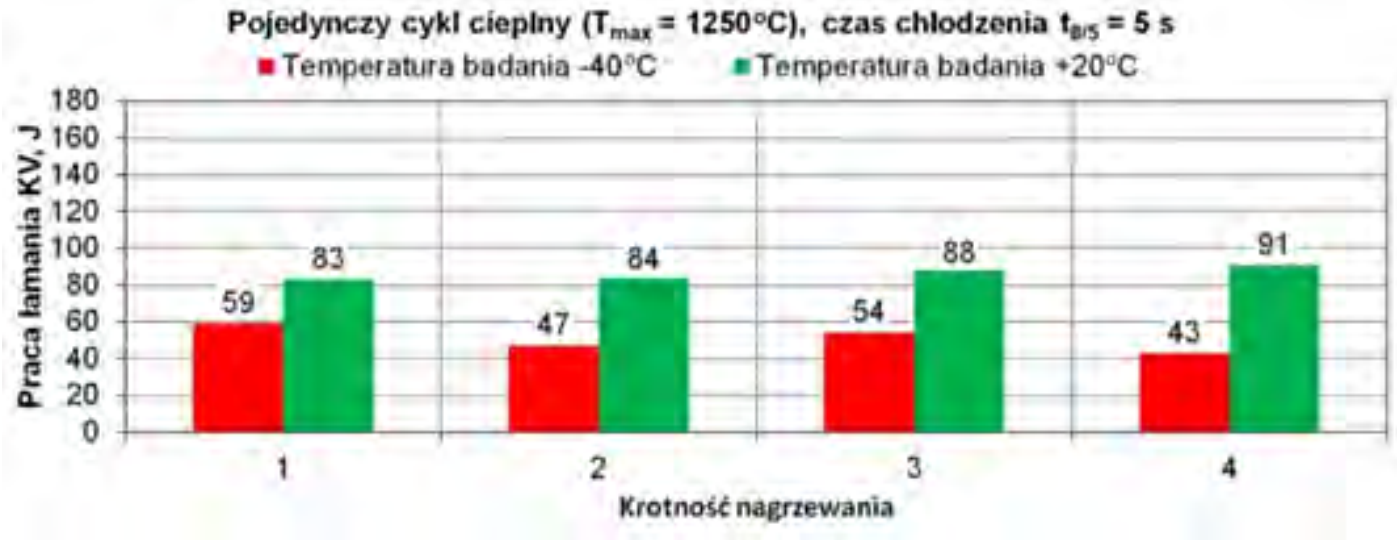

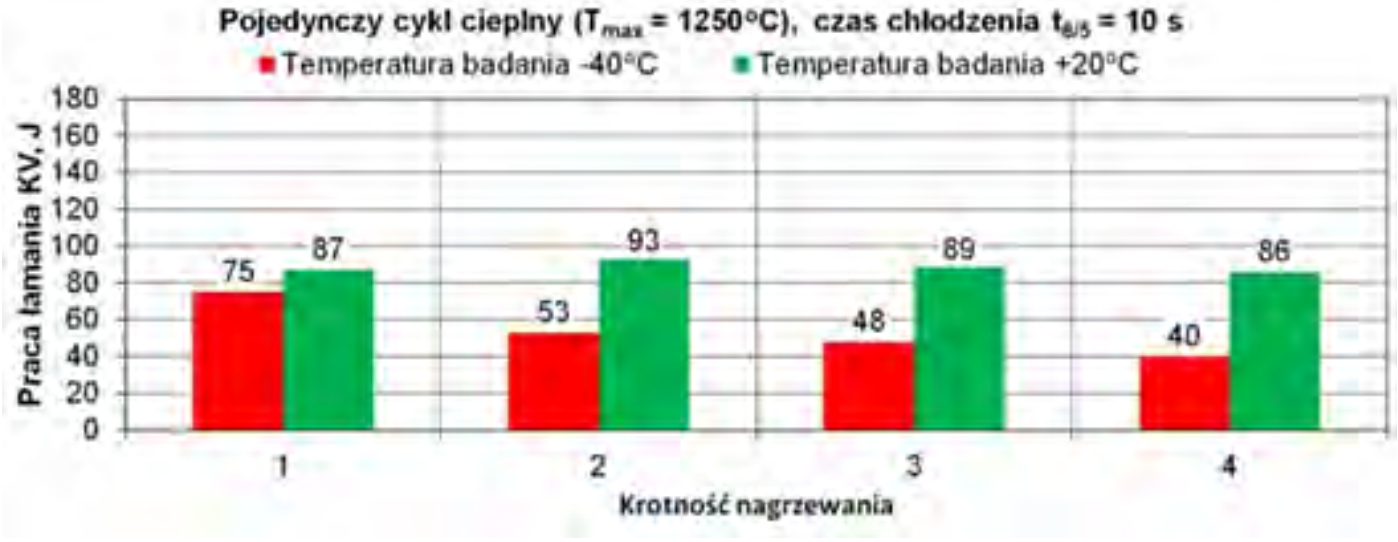

Fig. 13. Impact energy KV of the simulated HAZ areas of steel S1100QL in relation to the single thermal cycle in the function of the number of welding thermal cycles in relation to cooling time t8/5: a) 3 s, b) 5 s and c) 10 s

BY-NC

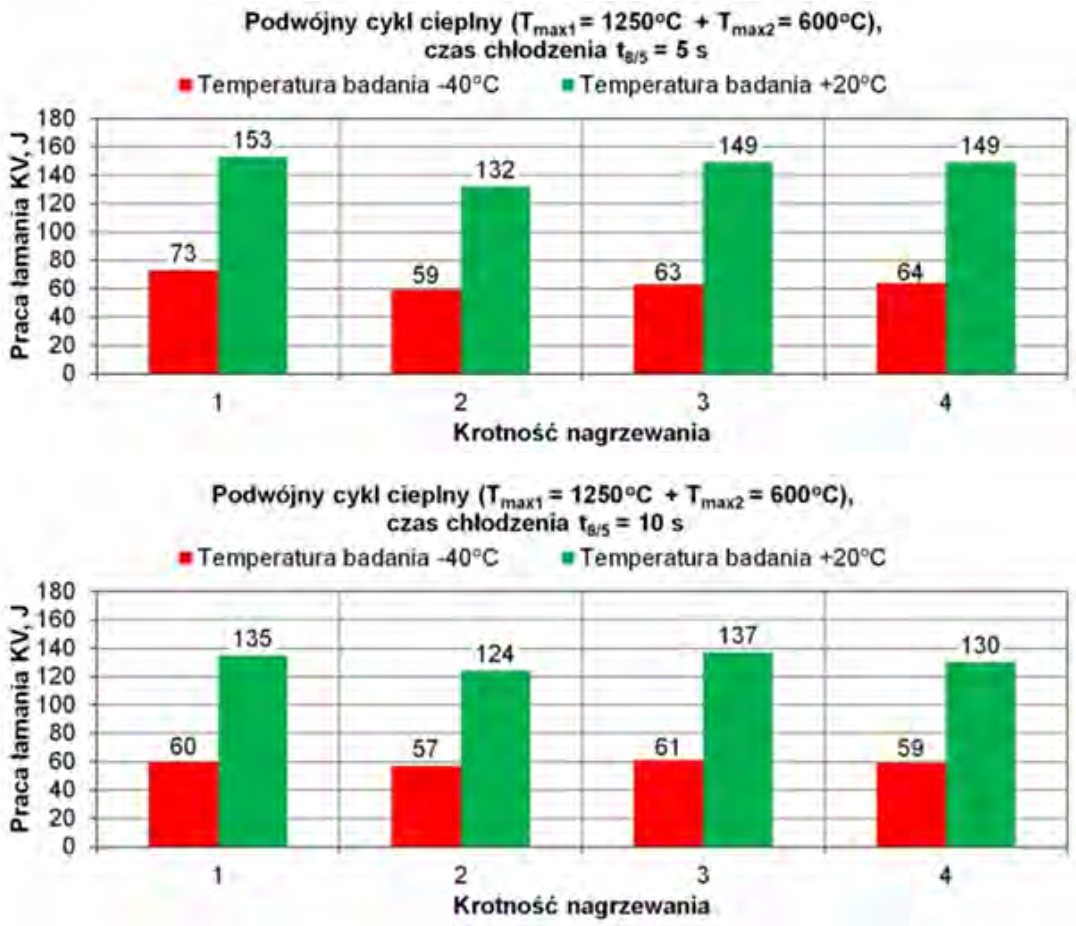

Fig. 14. Impact energy KV of the simulated HAZ areas of steel S1100QL in relation to the double thermal cycle (Tmax1 = 1250°C + Tmax2 = 600°C) in the function of the number of welding thermal cycles in relation to cooling time t8/5: a) 5 s and b) 10 s

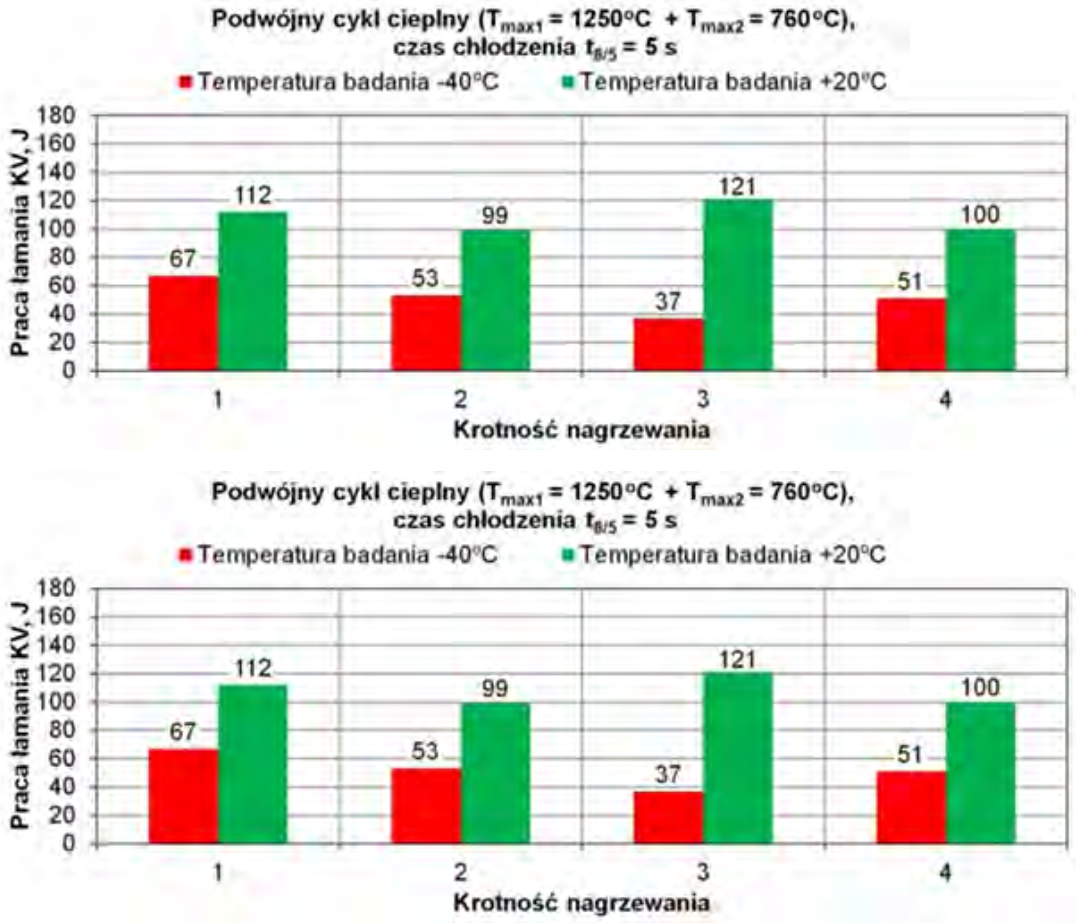

Fig. 15. Impact energy KV of the simulated HAZ areas of steel S1100QL in relation to the double thermal cycle (Tmax1 = 1250°C + Tmax2 = 760°C) in the function of the number of welding thermal cycles in relation to cooling time t8/5: a) 5 s and b) 10 s

BY-NC

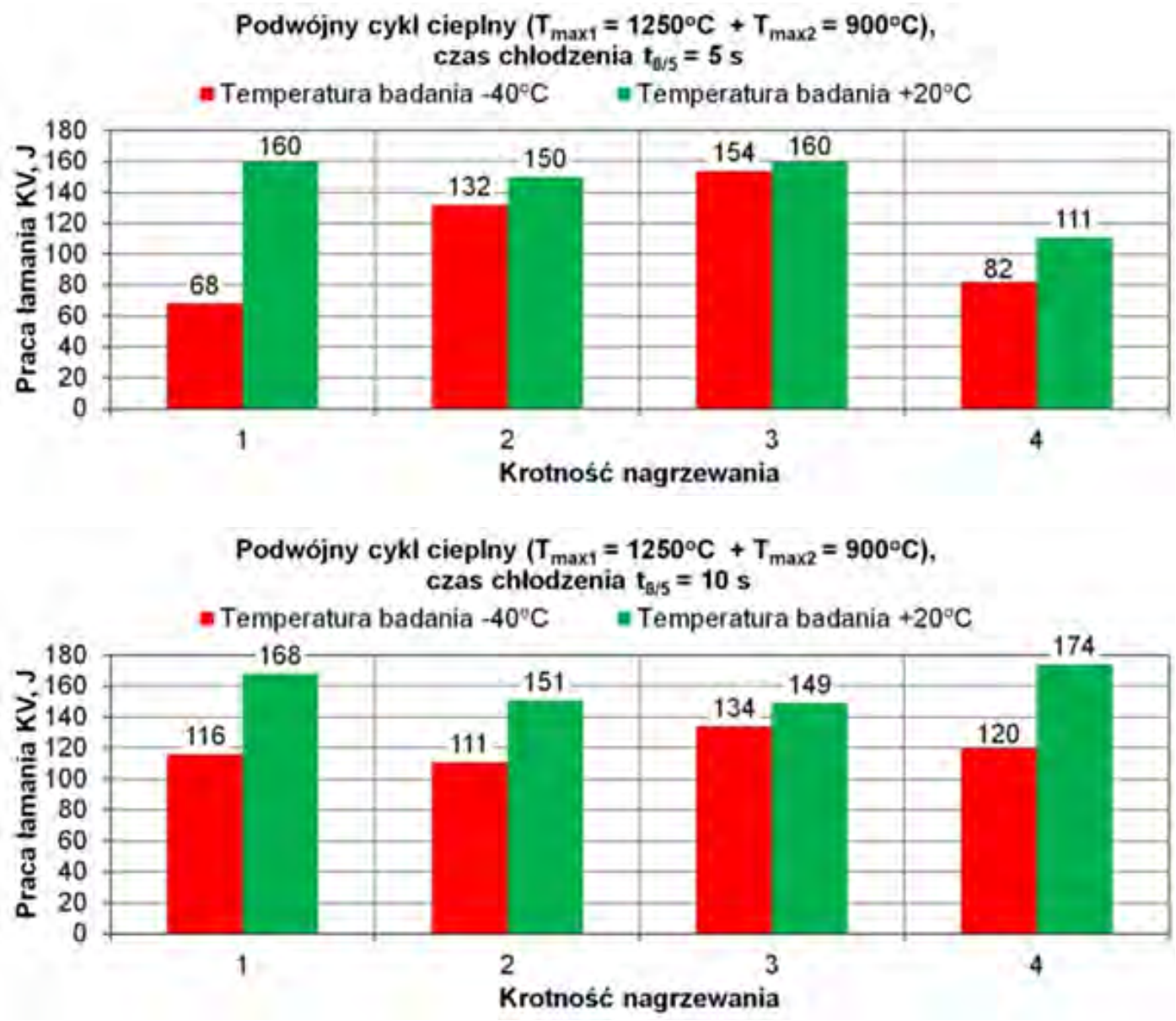

Fig. 16. Impact energy KV of the simulated HAZ areas of steel S1100QL in relation to the double thermal cycle (Tmax1 = 1250°C + Tmax2 = 900°C) in the function of the number of welding thermal cycles in relation to cooling time t8/5: a) 5 s and b) 10 s

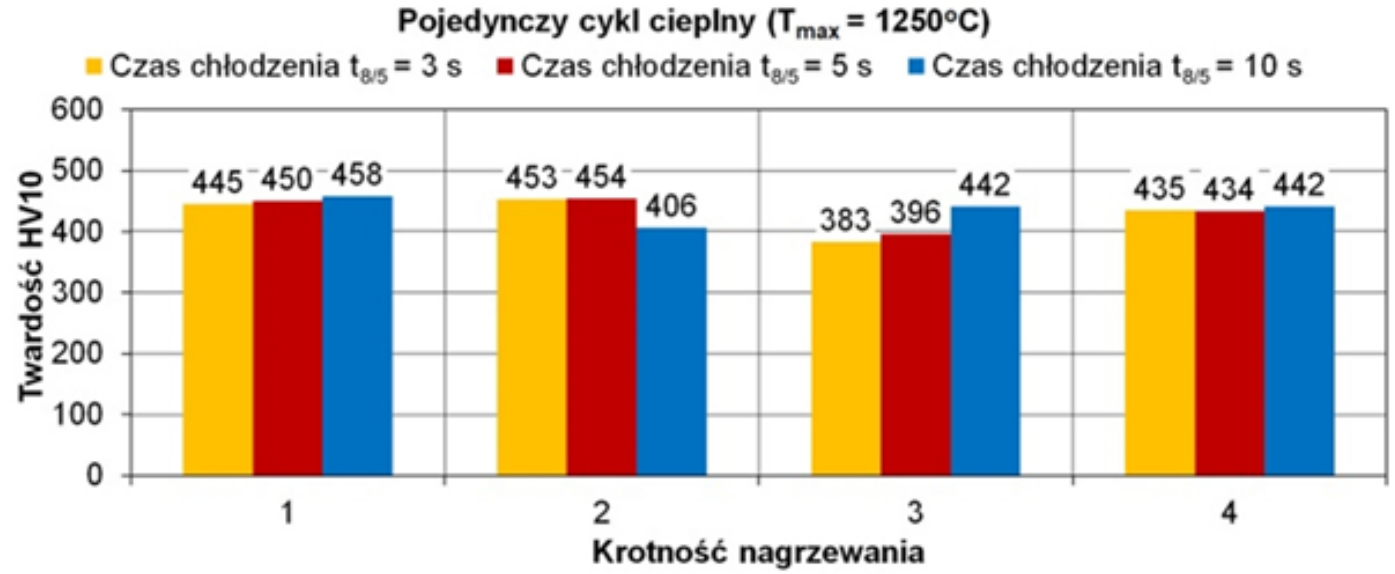

Fig. 17. Average values of hardness HV10 in relation to the simulated SWC areas of steel S1100QL in relation to the single thermal cycle Tmax = 1250°C in the function of the number of welding thermal cycles in relation to cooling time t8/5 = 3 s, 5 s and 10 s

BY-NC

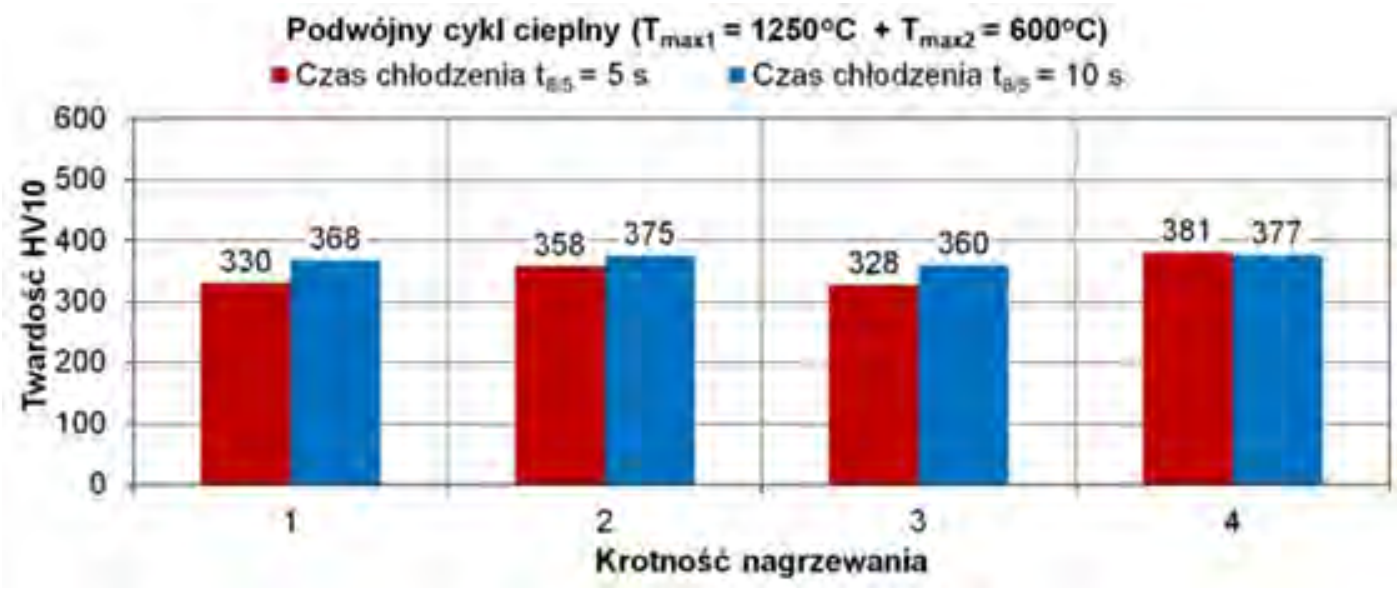

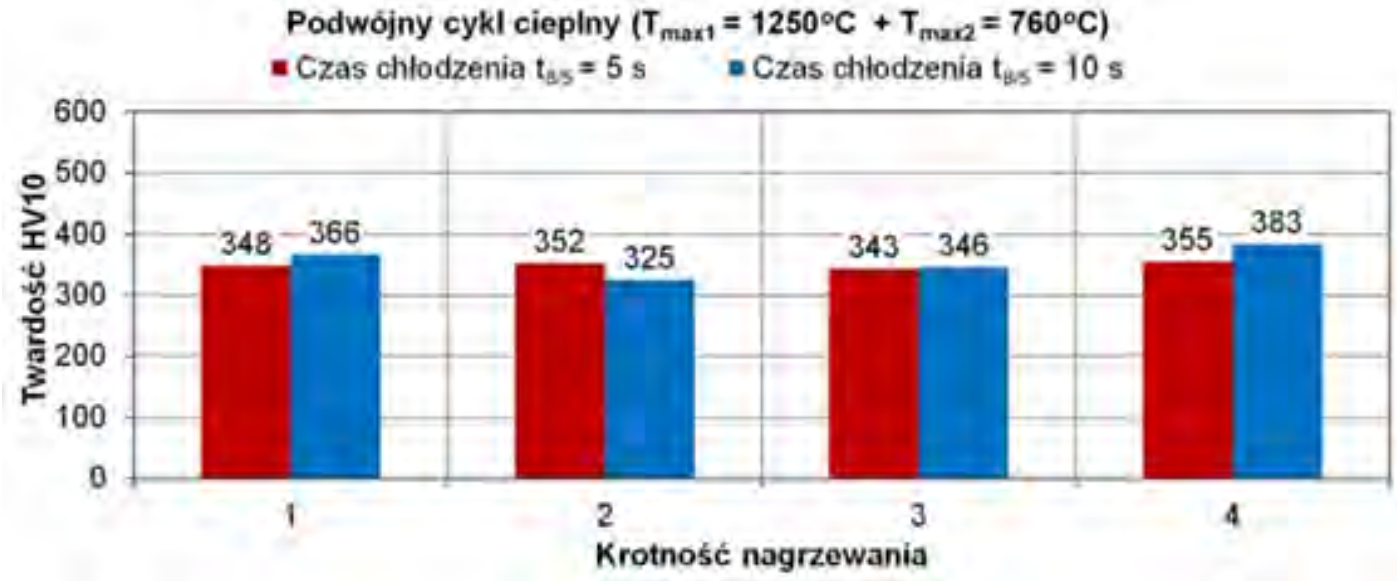

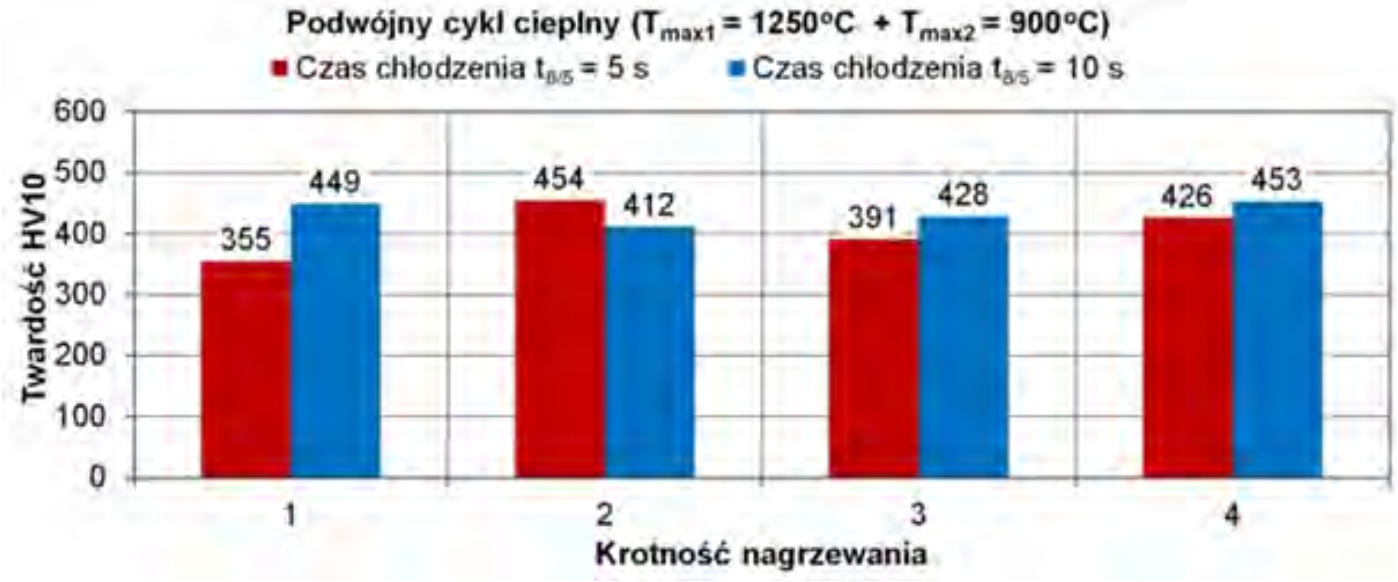

Fig. 18. Average values of hardness HV10 in relation to the simulated SWC areas of steel S1100QL in relation to cooling time t8/5 = 5 s and 10 s in the function of the number of welding thermal cycles in relation to double thermal cycles: a) Tmax1 = 1250°C + Tmax2 = 600°C, b) Tmax1 = 1250°C + Tmax2 = 760°C and c) Tmax1 = 1250°C + Tmax2 = 900°C

BY-NC

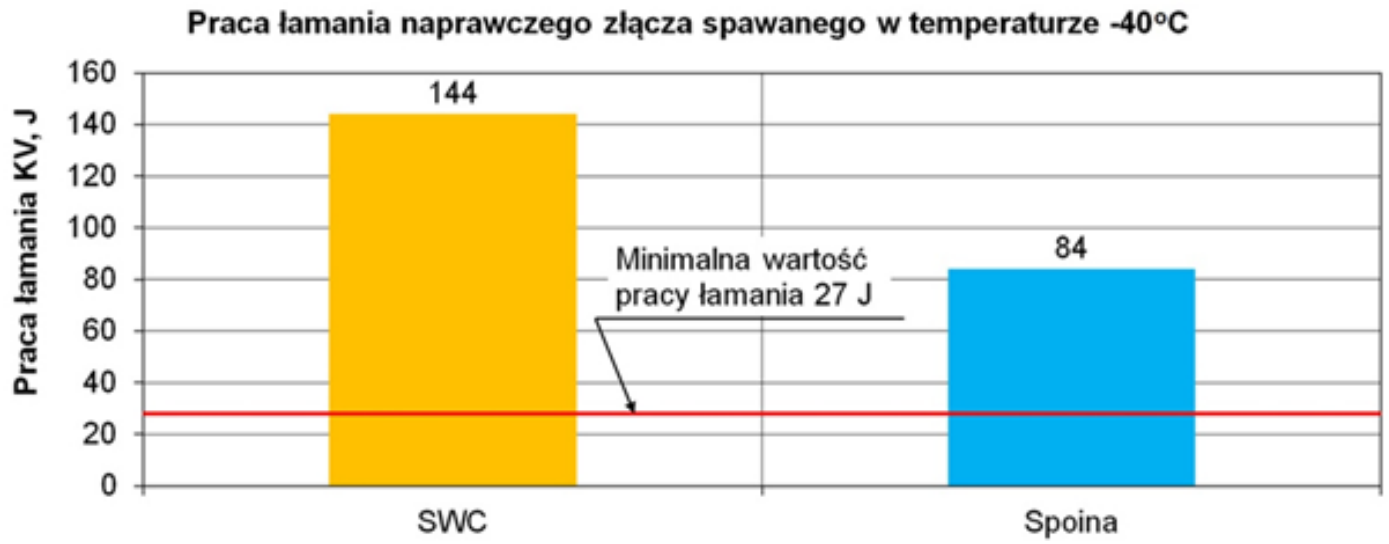

Fig. 19. Impact energy test results in relation to the repair joint

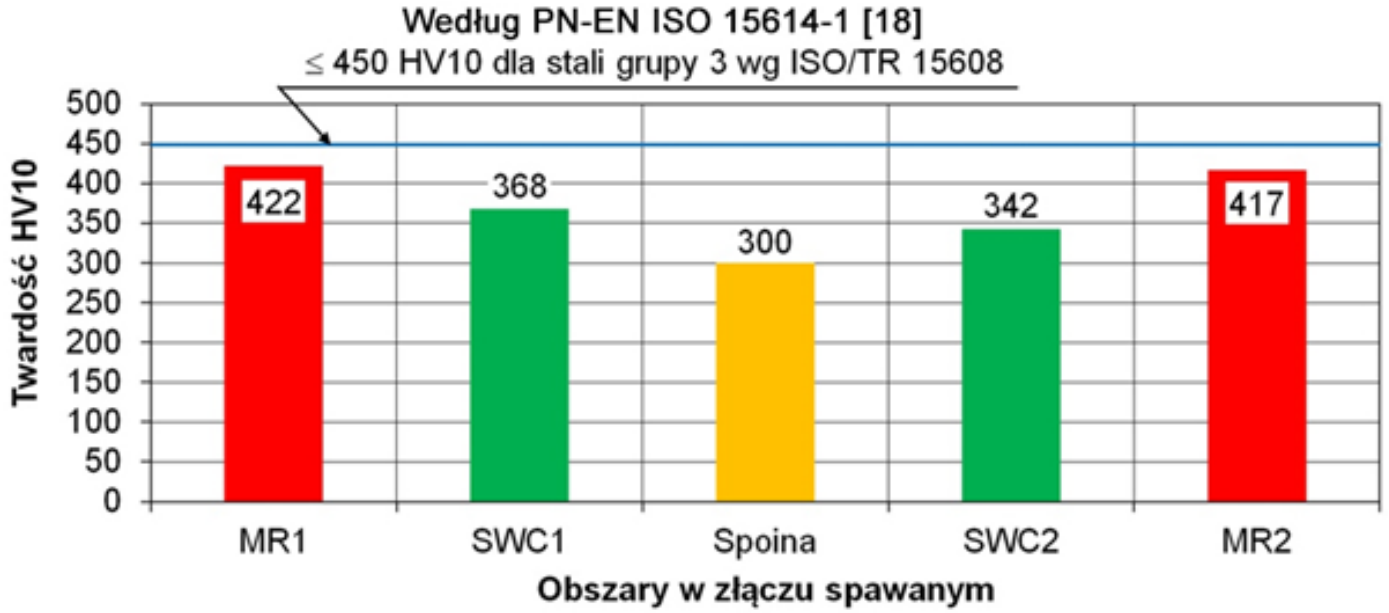

Fig. 20. Hardness measurement results related to the repair welded joint

Destructive test results concerning the welded joint subjected to quadruple repair

Impact energy test results as well as hardness measurement results concerning the repair welded joint are presented in Figures 19 and 20.

The macrostructure of the repair welded joint is presented in Figure 21. The results of the microscopic metallographic tests concerning the HAZ areas and the weld areas of the joint are presented in Figure 22.

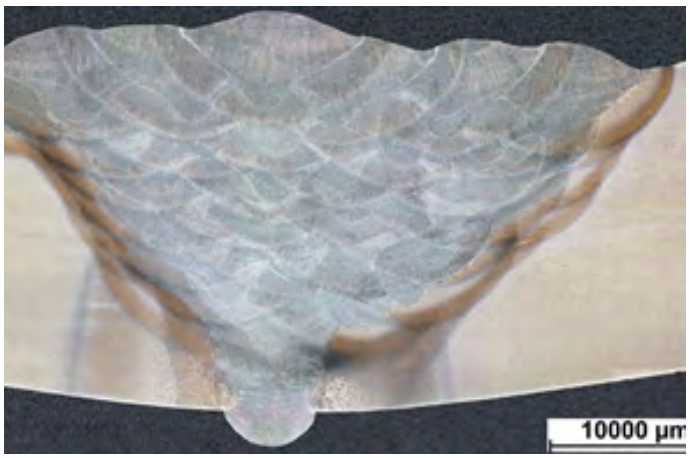

Fig. 21. Macrostructure of the welded joint after four repairs

BY-NC

Joint area	HAZ	Weld
At the weld face height	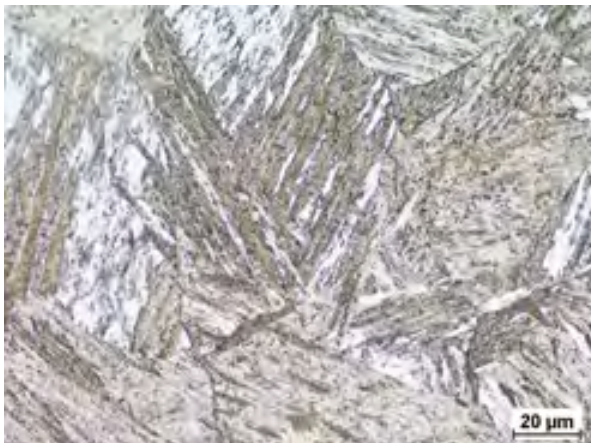	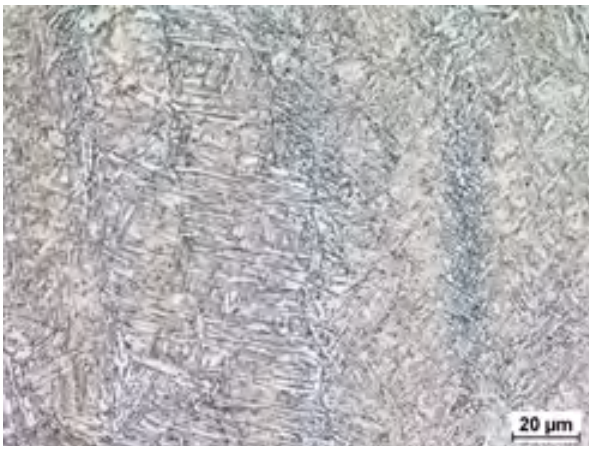
	Martensite; hardness: 387 HV10av.; mag. 500x	Mixture of bainite, small amounts of martensite and small amounts of ferrite; hardness: 311 HV10av.; mag. 500x
At the half of the joint thickness	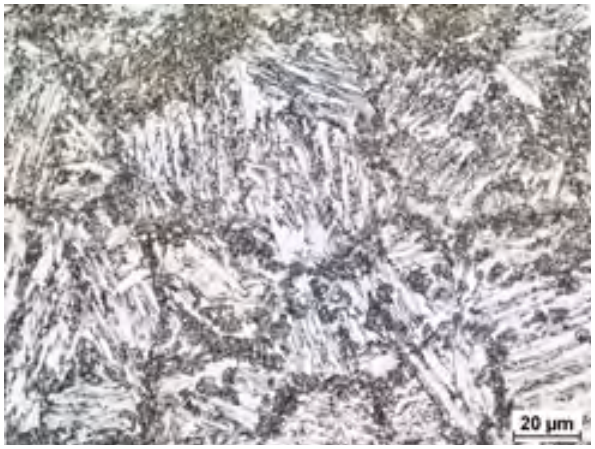	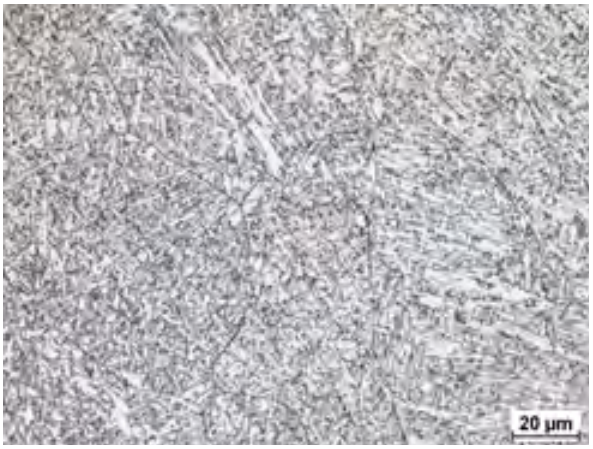
	Mixture of high-tempered martensite and "fresh" martensite along grain boundaries; hardness: 357 HV10av.; ,mag. 500x	Mixture of bainite and small amounts of ferrite; hardness: 314 HV10av.; mag. 500x
Near the weld root		
	Mixture of bainite, martensite and small amounts of ferrite; hardness: 359 HV10av. ; mag. 500x	Mixture of bainite and ferrite; hardness: 274 HV10av.; mag. 500x

Fig. 22. Microstructure of the HAZ areas and weld areas in the repair welded joint made of steel S1100QL, subjected to quadruple repair

BY-NC

Discussion

The microstructure of the base material of steel S1100QL contained martensite having an average hardness of 430 HV10av. (Fig. 3). In terms of all of the variants related to the single thermal cycle, the microstructure of the simulated HAZ areas of steel S1100QL contained martensite having characterised by average hardness restricted within the range of 383 HV10av. to 458 HV10av. (Fig. 4–6).

In terms of all of the variants related to the double thermal cycle (Tmax1 = 1250°C + Tmax2 = 600°C), the microstructure of the simulated HAZ areas of steel S1100QL contained the mixture of bainite and ferrite characterised by average hardness restricted within the range of 328 HV10av. to 381 HV10av. (Fig. 7–8).

As regards the double thermal cycle (Tmax1 = 1250°C + Tmax2 = 760°C), cooling time t8/5 = 5 s as well as the single and double heating, the microstructure of the simulated HAZ areas contained the mixture of bainite and ferrite characterised by an average hardness of 348 HV10av. and 352 HV10av. respectively (Fig. 9). After the third and the fourth repetition of the welding thermal cycle, in addition to bainite and ferrite, the microstructure (along grain boundaries) contained the so-called "fresh" martensite. The "fresh" martensite was formed from austenite (precipitated along grain boundaries) as a result of the exceeding temperature AC1 during the second thermal cycle. In relation to steel S1100QL, the value of temperature AC1 amounted to 700°C. The average hardness value related to the third and fourth heating amounted to 343 HV10av. and 355 HV10av. respectively (Fig. 9).

As regards the double thermal cycle (Tmax1 = 1250°C + Tmax2 = 760°C), cooling time t8/5 = 10 s as well as the single and double heating, the microstructure of the simulated HAZ areas contained the mixture of high-tempered martensite and "fresh" martensite along grain boundaries characterised by an average hardness of 366 HV10av. and 325 HV10av. respectively (Fig. 10). After the triple and quadruple repetition of heating, the microstructure of the HAZ area contained the mixture of bainite, martensite and ferrite. The average hardness values were 346 HV10av. and 383 HV10av. respectively (Fig. 10).

As regards to all the repetitions of heating in relation to the double thermal cycle (Tmax1 = 1250°C + Tmax2 = 900°C), the microstructure of the simulated HAZ areas contained the mixture of martensite, bainite and small amounts of ferrite (Fig. 11 and 12). In relation to cooling time t8/5 = 5 s, the average hardness values were restricted within the range of 355 HV10av. to 454 HV10av. (Fig. 11). In turn, in relation to cooling time t8/5 = 10 s, the average hardness values were restricted within the range of 412 HV10av. to 453 HV10av. (Fig. 12).

The test results regarding the average impact energy values concerning the simulated HAZ areas of steel S1100QL (presented in Figures 13–16) revealed that all of the simulation variants, (related a testing temperature of -40°C and that of +20°C) satisfied the required criterion of 27 J.

The test results regarding the average impact energy values concerning the simulated HAZ areas of steel S1100QL in relation to the single thermal cycle (Tmax = 1250°C; Fig. 17) revealed that the lowest hardness value of 383 HV10av. was obtained in relation to triple heating and cooling time t8/5 = 3 s. In turn, the highest hardness value of 458 HV10av. was obtained in relation to single heating and cooling time t8/5 = 10 s.

As regards the double thermal cycle (Tmax1 = 1250°C + Tmax2 = 600°C), the lowest hardness value of 328 HV10av. was obtained in relation to triple heating and cooling time t8/5 = 5 s. In turn, the highest hardness value of 381 HV10av. was obtained in relation to quadruple heating and cooling time t8/5 = 15 s (Fig. 18a).

As regards the double thermal cycle (Tmax1 = 1250°C + Tmax2 = 760°C) the lowest hardness value of 325 HV10av. was obtained in relation to double heating and cooling time t8/5 =

BY-NC

10 s. In turn, the highest hardness value of 383 HV10av. was obtained in relation to quadruple heating and cooling time t8/5 = 10 s (Fig. 18b).

As regards the double thermal cycle (Tmax1 = 1250°C + Tmax2 = 900°C) the lowest hardness value of 355 HV10av. was obtained in relation to single heating and cooling time t8/5 = 5 s. In turn, the highest hardness value of 454 HV10av. was obtained in relation to quadruple heating and cooling time t8/5 = 5 s (Fig. 18c).

The tests concerning the steel with the simulated HAZ revealed specific trends as regards changes in the microstructure of the steel and its mechanical properties (hardness and toughness). It is expected that steels such as S1100QL should be characterised by high strength, high yield point (in particular) as well as favourable toughness at lower temperature. The appropriate combination of high toughness and high hardness of the simulated HAZ of steel S1100QL was obtained using the single thermal cycle in relation maximum temperature Tmax = 1250°C, all cooling times, i.e. t8/5 = 3 s, 5 s and 10 s and all repetitions of the heating process as well as the double thermal cycle Tmax1 = 1250°C + Tmax2 = 900°C in relation to both cooling times, i.e. t8/5 = 5 s and 10 s and the number of the repetitions of the heating process restricted within the range of 1 to 4.

The comparison of the microscopic metallographic test results of the simulated HAZ areas with those in the actual welded joint revealed

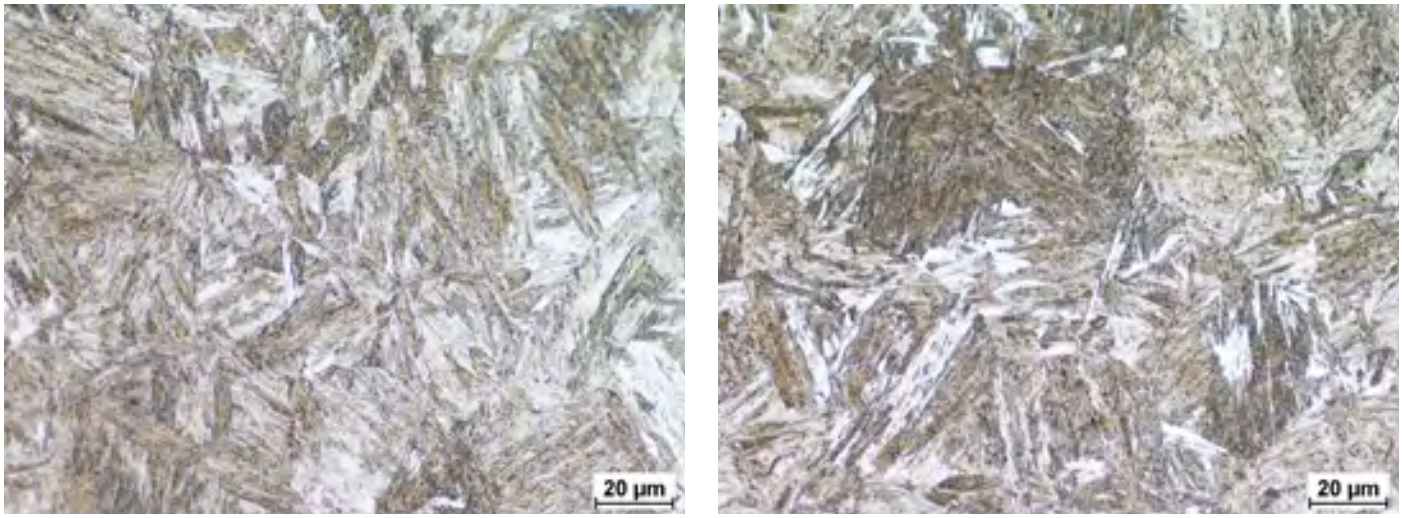

Fig. 23. HAZ area at the weld face height; martensite: a) area after the simulated cycle Tmax = 1250°C, t8/5 = 3 s, hardness: 383 HV10av. and b) repair welded joint; hardness: 387 HV10av.; etchant: Nital, mag. 500x

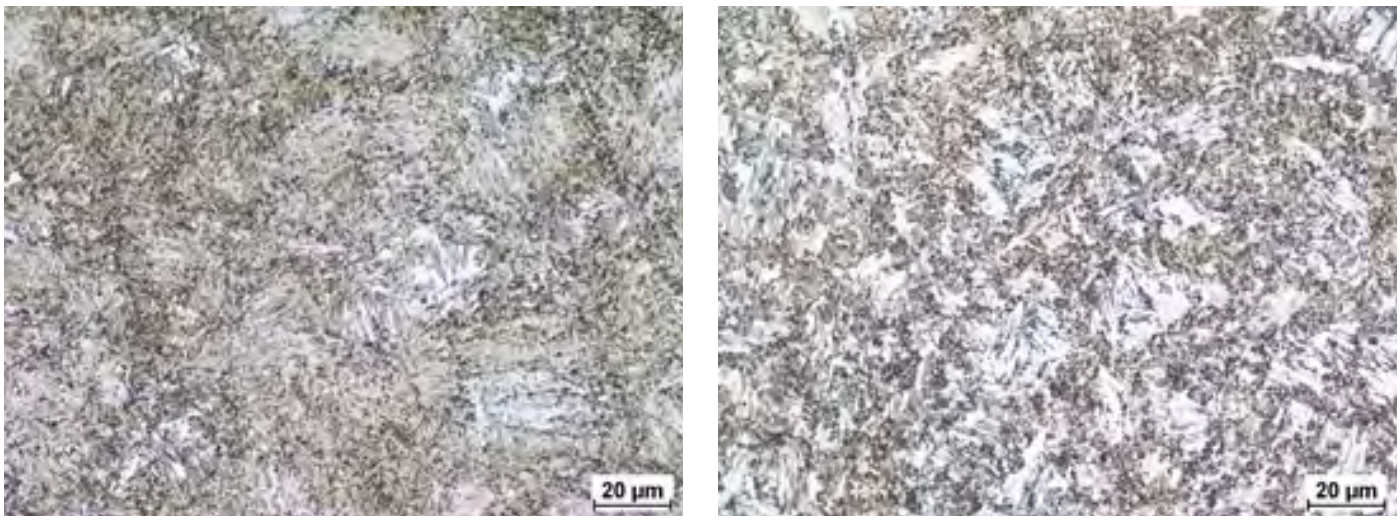

Fig. 24. HAZ area at the half of the joint thickness; mixture of high-tempered martensite, "fresh" martensite along grain boundaries and small amounts of ferrite: a) area after the simulated cycle Tmax = 1250 + 760°C, t8/5 = 10 s, hardness: 366 HV10av. and b) repair welded joint; hardness: 357 HV10av.; etchant: Nital, mag. 500x

BY-NC

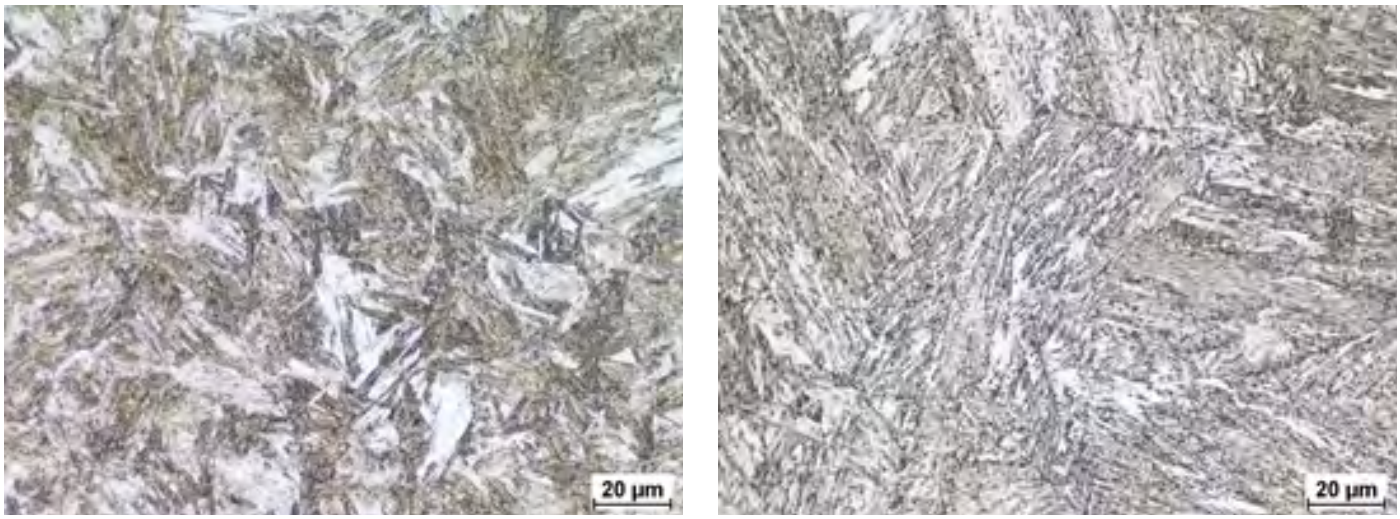

Fig. 25. HAZ area near the weld root; mixture of bainite, martensite and small amounts of ferrite: a) area after the simulated cycle Tmax = 1250 + 760°C, t8/5 = 5 s, hardness: 348 HV10av. and b) repair welded joints, hardness: 359 HV10av.; etchant: Nital, mag. 500x

the significance similarity both in terms of the microstructure morphology and hardness values (see Figures 23–25).

Conclusions

The above-presented tests and their results justified the formulation of the following conclusions:

1. Depending on the thermal cycle variants, the microstructure of the simulated HAZ area of steel underwent changes of its composition ranging from martensite in relation to the single thermal cycle, through the mixture of bainite and martensite in relation to the double cycle Tmax1 = 1250°C + Tmax2 = 600°C as well as the mixture of high-tempered martensite and "fresh" martensite along grain boundaries in relation to the double cycle Tmax1 = 1250°C + Tmax2 = 760°C to the mixture of martensite, bainite and small amounts of ferrite in relation to the double cycle Tmax1 = 1250°C + Tmax2 = 900°C.
2. The microscopic observations demonstrated high similarity between the phase composition, microstructural morphology and average hardness values as regards the simulated HAZ areas and the HAZ of the repair welded joint.
3. In terms of all the simulation variants, the impact energy of the simulated HAZ area of steel satisfied the minimum criterion KV = 27 J and was restricted within the range of 34 J to 154 J in relation to a testing temperature of -40°C and within the range of 83 J to 174 J in relation to a testing temperature of +20°C.
4. In terms of steel S1100QL, the number of the repetitions of the thermal cycle of preset parameters (between single and quadruple heating) did not trigger any clearly noticeable tendency as regards changes in the impact every values related to the simulated HAZ areas.
5. The recommended thermal cycle enabling the obtainment of the appropriate combination of the high toughness and high hardness of the simulated HAZ areas of steel S1100QL (being similar to the hardness of the base material of the steel) was the single thermal cycle of the maximum temperature Tmax = 1250°C in relation to all cooling times, i.e. t8/5 = 3 s, 5 s and 10 s and all and all repetitions of the heating process as well as the double thermal cycle Tmax1 = 1250°C + Tmax2 = 900°C in relation to both cooling times, i.e. t8/5 = 5 s and 10 s and the number of the repetitions of the heating process restricted within the range of 1 to 4.

BY-NC

References

[1] Węglowski M. St., Zeman M.: Spawalność Stali WELDOX o granicy plastyczności 1300 MPa. Seminarium Instytutu Spawalnictwa pt. „Nowoczesne stale do pracy w ekstremalnych warunkach eksploatacyjnych", 19.04.2012.

[2] Zeman M.: Spawalność ulepszonej cieplnie stali o granicy plastyczności 1100 MPa. Seminarium Instytutu Spawalnictwa pt. „Nowoczesne stale do pracy w ekstremalnych warunkach eksploatacyjnych", 19.04.2012.

[3] Kaha P., Pirinen M., Suoranta R., Martikainen J.: Welding of Ultra High Strength Steels. Advanced Materials Research, 2014, vol. 849, pp. 357–365.

[4] STRENX Performance Steel. Strenx 1300. SSAB. Data sheet 2020 Strenx 1300, 2016-04-12.

[5] STRENX Performance Steel. Welding of Strenx. SSAB. 2017.

[6] Nowacki J., Sajek A., Matkowski P.: The influence of welding heat input on the microstructure of joints of S1100QL steel in one-pass welding. Archives of Civil and Mechanical Engineering, 2016, vol. 16, pp. 777–783.

[7] Holly S., Haslberger Ph., Zügner D., Schnitzer R., Kozeschnik E.: Development of high-strength welding consumables using calculations and microstructural characterisation. Welding in the World, 2018, vol. 62, pp. 451–458.

[8] Haslberger Ph., Holly S., Ernst W., Schnitzer R.: Microstructure and Mechanical Properties of high-strength steel welding consumables with a minimum yield strength of 1100 MPA. J. Mater. Sci., 2018, vol. 53, pp. 6968–6979.

[9] Engindeniz E.: MAG welding of high strength special-purpose structural steel with Flux cored wires. Drahtzug Stein, 2015.

[10] Brochure by SSAB: Strenx 1100. SSAB. Data sheet Strenx 1100, 2017-04-20.

[11] Mikuła J.: Analityczne metody oceny spawalności stali. Zeszyty Naukowe Politechniki Krakowskiej, p. Mechanika, no. 85, Kraków 2001.

[12] Zeman M.: Analiza stanu zagadnienia i ukierunkowanie badań wraz z praktycznymi przykładami zastosowań metod matematycznych w analizowanym zakresie. Praca badawcza Instytutu Spawalnictwa, Hc-60 (C-31.3.4), CPBR 7.3 „Techniki spawalnicze", 1987.

[13] PN-EN ISO 148-1:2017-02 Metale. Próba udarności sposobem Charpy'ego. Część 1: Metoda badania.

[14] PN-EN ISO 17639:2013-12 Badania niszczące spawanych złączy metali. Badania makroskopowe i mikroskopowe złączy spawanych.

[15] PN-EN ISO 6507-1:2018-05 Metale. Pomiar twardości sposobem Vickersa. Część 1: Metoda badania.

[16] PN-EN ISO 9016:2013-05 Badania niszczące złączy spawanych metali. Badanie udarności. Usytuowanie próbek, kierunek karbu i badanie.

[17] PN-EN ISO 9015-1:2011 Badania niszczące złączy spawanych metali. Badanie twardości. Część 1: Badanie twardości złączy spawanych łukowo.

[18] PN-EN ISO 15614-1:2017-08 Specyfikacja i kwalifikowanie technologii spawania metali. Badanie technologii spawania. Część 1: Spawanie łukowe i gazowe stali oraz spawanie łukowe niklu i stopów niklu.